Magnetism and thermodynamics of spin-1/2 Heisenberg diamond chains in a magnetic field

Bo Gu and Gang Su*

College of Physical Sciences, Graduate University of Chinese Academy of Sciences, P.O. Box 4588, Beijing 100049, China

(Received 5 October 2006; revised manuscript received 19 March 2007; published 24 May 2007)

The magnetic and thermodynamic properties of spin-1/2 Heisenberg diamond chains are investigated in three different cases: (a) $J_1, J_2, J_3>0$ (frustrated), (b) $J_1, J_3<0, J_2>0$ (frustrated), and (c) $J_1, J_2>0, J_3<0$ (nonfrustrated), where the bond coupling J_i $(i=1,2,3)>0$ stands for an antiferromagnetic (AF) interaction, and <0 for a ferromagnetic (F) interaction. The density-matrix renormalization-group (DMRG) technique is invoked to study the properties of the system in the ground state, while the transfer-matrix renormalization-group (TMRG) technique is applied to explore the thermodynamic properties. The local magnetic moments, spin-correlation functions, and static structure factors are discussed in the ground state for the three cases. It is shown that the static structure factor $S(q)$ shows peaks at wave vectors $q=a\pi/3$ $(a=0,1,2,3,4,5)$ for different couplings in a zero magnetic field, which, however, in the magnetic fields where the magnetization plateau with $m=1/6$ pertains, exhibits the peaks only at $q=0$, $2\pi/3$, and $4\pi/3$, which are found to be couplings independent. The DMRG results of the zero-field static structure factor can be nicely fitted by a linear superposition of six modes, where two fitting equations are proposed. It is observed that the six modes are closely related to the low-lying excitations of the system. At finite temperatures, the magnetization, susceptibility, and specific heat show various behaviors for different couplings. The double-peak structures of the susceptibility, and specific heat against temperature are obtained, where the peak positions and heights are found to depend on the competition of the couplings. It is also uncovered that the *XXZ* anisotropy of F and AF couplings leads the system of case (c) to display quite different behaviors. In addition, the experimental data of the susceptibility, specific heat, and magnetization for the compound $Cu_3(CO_3)_2(OH)_2$ are fairly compared with our TMRG results.

DOI: 10.1103/PhysRevB.75.174437 PACS number(s): 75.10.Jm, 75.40.Cx

I. INTRODUCTION

Low-dimensional quantum spin systems with competing interactions have become an intriguing subject in the last decades. Among many achievements in this area, the phenomenon of the topological quantization of magnetization has attracted much attention both theoretically and experimentally. A general necessary condition for the appearance of the magnetization plateaus has been proposed by Oshikawa, Yamanaka, and Affleck (OYA),[1] stating that for the Heisenberg antiferromagnetic (AF) spin chain with a single-ion anisotropy, the magnetization curve may have plateaus at which the magnetization per site m is topologically quantized by $n(S-m)=integer$, where S is the spin and n is the period of the ground state determined by the explicit spatial structure of the Hamiltonian. As one of fascinating models which potentially possesses the magnetization plateaus, the Heisenberg diamond chain, consisting of diamond-shaped topological unit along the chain, as shown in Fig. 1, has also gained much attention both experimentally and theoretically (e.g., Refs. 2–15).

It has been observed that the compounds, $A_3Cu_3(PO_4)_4$ with $A=Ca$, Sr^2, and $Bi_4Cu_3V_2O_{14}$ (Ref. 3) can be nicely modeled by the Heisenberg diamond chain. Another spin-1/2 compound $Cu_3Cl_6(H_2O)_2\cdot 2H_8C_4SO_2$ was initially regarded as a model substance for the spin-1/2 diamond chain,[4] but a later experimental research reveals that this compound should be described by a double chain model with very weak bond alternations, and the lattice of the compound is found to be $Cu_2Cl_4\cdot H_8C_4SO_2$.[5] Recently, Kikuchi *et al.*[6] have reported the experimental results on a spin-1/2 compound $Cu_3(CO_3)_2(OH)_2$, where local Cu^{2+} ions with spin $S=1/2$ are arranged along the chain direction, and the diamond-shaped units consist of a one-dimensional (1D) lattice. The 1/3 magnetization plateau and the double peaks in the magnetic susceptibility as well as the specific heat as functions of temperature have been observed experimentally[6,7] and have been discussed in terms of the spin-1/2 Heisenberg diamond chain with AF couplings J_1, J_2, and $J_3>0$.

On the theoretical aspect, the frustrated diamond spin chain with AF interactions J_1, J_2, and $J_3>0$ was studied by a few groups. The first diamond spin chain was explored under a symmetrical condition $J_1=J_3$.[8] Owing to the competition of AF interactions, the phase diagram in the ground state of the spin-1/2 frustrated diamond chain was found to contain different phases, in which the magnetization plateaus at m

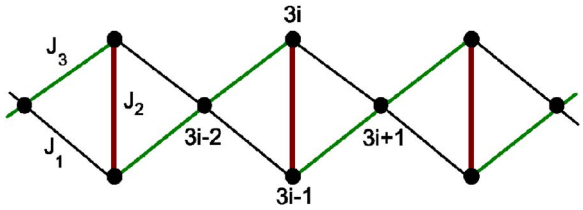

FIG. 1. (Color online) Sketch of the Heisenberg diamond chain. The bond interactions are denoted by J_1, J_2, and J_3. Three cases will be considered: (a) $J_1, J_2, J_3>0$ (a frustrated diamond chain), (b) $J_1, J_3<0, J_2>0$ (a frustrated diamond chain with competing interactions), and (c) $J_1, J_2>0, J_3<0$ (a diamond chain without frustration). Note that $J_i>0$ stands for an antiferromagnetic interaction while $J_i<0$ for a ferromagnetic interaction, where $i=1,2,3$.

$=1/6$ as well as $1/3$ are predicted.[9–13] Another frustrated diamond chain with ferromagnetic (F) interactions J_1 and $J_3<0$ and AF interaction $J_2>0$ was also investigated theoretically, which can be experimentally realized if all angles of the exchange coupling bonds are arranged to be around 90°, a region where it is usually hard to determine safely the coupling constants and even their signs.[14,15] Despite these works, the investigations on the Heisenberg diamond spin chain with various competing interactions are still sparse.

Motivated by the recent experimental observation on the azurite compound $Cu_3(CO_3)_2(OH)_2$,[6,7] we shall explore systematically the magnetic and thermodynamic properties of the spin-1/2 Heisenberg diamond chain with various competing interactions in a magnetic field and attempt to fit into the experimental observation on the azurite in a consistent manner. The density-matrix renormalization-group (DMRG) as well as the transfer-matrix renormalization-group (TMRG) techniques will be invoked to study the ground-state properties and thermodynamics of the model under interest, respectively. The local magnetic moments, spin-correlation functions, and static structure factors will be discussed for three cases at zero temperature. It is found that the static structure factor $S(q)$ shows peaks in zero magnetic field at wave vectors $q=a\pi/3$ $(a=0,1,2,3,4,5)$ for different couplings, while in the magnetic fields where the magnetization plateau with $m=1/6$ remains, the peaks appear only at wave vectors $q=0$, $2\pi/3$, and $4\pi/3$, which are found to be couplings independent. These information could be useful for further neutron studies. The double-peak structures of the susceptibility and specific heat against temperature are obtained, where the peak positions and heights are found to depend on the competition of the couplings. It is uncovered that the *XXZ* anisotropy of F and AF couplings leads the system without frustration (see below) to display quite different behaviors. In addition, the experimental data of the susceptibility, specific heat and magnetization for the compound $Cu_3(CO_3)_2(OH)_2$ are fairly compared with our TMRG results.

The rest of this paper is outlined as follows. In Sec. II, we shall introduce the model Hamiltonian for the spin-1/2 Heisenberg diamond chain with three couplings J_1, J_2, J_3, where three particular cases are identified. In Sec. III, the magnetic and thermodynamic properties of a frustrated diamond chain with AF interactions J_1, J_2, $J_3>0$ will be discussed. In Sec. IV, the physical properties of another frustrated diamond chain with F interactions J_1, $J_3<0$ and AF interaction $J_2>0$ will be considered. In Sec. V, the magnetism and thermodynamics of a nonfrustrated diamond chain with AF interactions J_1, $J_2>0$ and F interaction $J_3<0$ will be explored, and a comparison to the experimental data on the azurite compound will be made. Finally, a brief summary and discussion will be presented in Sec. VI.

II. MODEL

The Hamiltonian of the spin-1/2 Heisenberg diamond chain reads

$$\mathcal{H}=\sum_{i=1}^{L/3}(J_1\mathbf{S}_{3i-2}\cdot\mathbf{S}_{3i-1}+J_2\mathbf{S}_{3i-1}\cdot\mathbf{S}_{3i}+J_3\mathbf{S}_{3i-2}\cdot\mathbf{S}_{3i}+J_3\mathbf{S}_{3i-1}\cdot\mathbf{S}_{3i+1}+J_1\mathbf{S}_{3i}\cdot\mathbf{S}_{3i+1})-\mathbf{H}\cdot\sum_{j=1}^{L}\mathbf{S}_j, \quad (1)$$

where $\mathbf{S}_j$ is the spin operator at the jth site, L is the total number of spins in the diamond chain, J_i $(i=1,2,3)$ stands for exchange interactions, $\mathbf{H}$ is the external magnetic field, $g\mu_B=1$, and $k_B=1$. $J_i>0$ represents the AF coupling, while $J_i<0$ the F interaction. There are three different cases particularly interesting, as displayed in Fig. 1, which will be considered in the present paper: (a) a frustrated diamond chain with J_1, J_2, $J_3>0$, (b) a frustrated diamond chain with competing interactions J_1, $J_3<0$, $J_2>0$, and (c) a diamond chain without frustration with J_1, $J_2>0$, $J_3<0$. It should be remarked that in case (c) of this model, since the two end points of the J_2 bond represent the two different lattice sites, it is possible that J_1 and J_3 can be different, even in their signs.

The magnetic properties and thermodynamics for the aforementioned three spin-1/2 Heisenberg diamond chains in the ground states and at finite temperatures will be investigated by means of the DMRG and TMRG methods, respectively. As the DMRG and TMRG techniques were detailed in two nice reviews,[16,17] we shall not repeat the technical details to be concise. In the ground-state calculations, the total number of spins in the diamond chain is taken at least as $L=120$. At finite temperatures, the thermodynamic properties presented below are calculated down to temperature $T=0.05$ (in units of $|J_1|$) in the thermodynamic limit. In our calculations, the number of kept optimal states is taken as 81, the width of the imaginary time slice is taken as $\varepsilon=0.1$, the Trotter-Suzuki error is less than 10^{-3}, and the truncation error is smaller than 10^{-6}.

III. A FRUSTRATED HEISENBERG DIAMOND CHAIN ($J_1,J_2,J_3>0$)

A. Local magnetic moment and spin-correlation function

Figure 2(a) manifests the magnetization process of a frustrated spin-1/2 Heisenberg diamond chain with the couplings satisfying $J_1:J_2:J_3=1:2:2$ at zero temperature. The plateau of magnetization per site $m=1/6$ is observed. According to the OYA necessary condition,[1] the $m=1/6$ plateau of a spin-1/2 Heisenberg chain corresponds to the period of the ground state $n=3$. Beyond the magnetization plateau region, the magnetic curve goes up quickly with the increasing magnetic field H. Above the upper critical field, the magnetic curve shows a s-like shape. To further look at how this magnetization plateau appears, the spatial dependence of the averaged local magnetic moment $\langle S_j^z\rangle$ in the ground states under different external fields is presented, as shown in Fig. 2(b). It is seen that in the absence of external field, the expectation value $\langle S_j^z\rangle$ changes its sign at every three sites within a very small range of $(-10^{-3},10^{-3})$ because of quan-

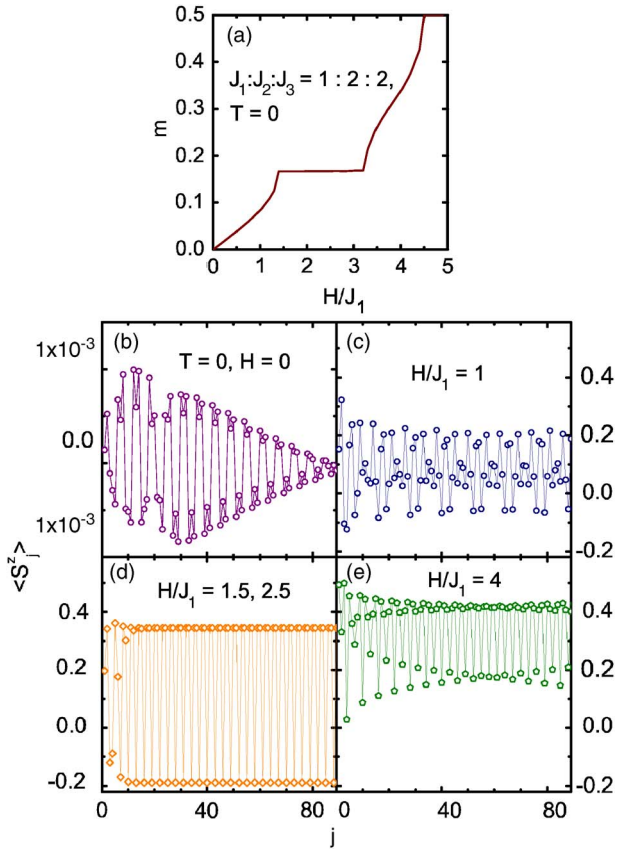

FIG. 2. (Color online) For a spin-1/2 frustrated Heisenberg diamond chain with fixed couplings $J_1:J_2:J_3=1:2:2$, (a) the magnetization per site m as a function of magnetic field H in the ground states, and the spatial dependence of the averaged local magnetic moment $\langle S_j^z\rangle$ in the ground states with external field (b) $H/J_1=0$, (c) 1, (d) 1.5 and 2.5, and (e) 4.

tum fluctuations, resulting in the magnetization per site $m=\Sigma_{j=1}^{L}\langle S_j^z\rangle/L=0$. $\langle S_j^z\rangle$ increases with the increasing magnetic field, and oscillates with increasing j, whose unit of three spins is gradually divided into a pair and a single, as displayed in Fig. 2(c). At the field $H/J_1=1.5$, as demonstrated in Fig. 2(d), the behavior of $\langle S_j^z\rangle$ falls into a perfect sequence such as $\{\ldots,(S_a,S_a,S_b),\ldots\}$ with $S_a=0.345$ and $S_b=-0.190$, giving rise to the magnetization per site $m=1/6$. In addition, such a sequence remains with the increasing magnetic field until $H/J_1=2.5$, implying that the $m=1/6$ plateau appears in the range of $H/J_1=1.5-2.5$, as manifested in Fig. 2(a). When the field is promoted further, the sequence changes into a waved succession with a smaller swing of (S_a-S_b), as shown in Fig. 2(e), which corresponds to the fact that the plateau state of $m=1/6$ is destroyed, and gives rise to a s-like shape of $M(H)$. It is noting that when the plateau state of $m=1/6$ is destroyed, the increase of m at first is mainly attributed to a rapid lift of S_b, and later, the double S_a start to flimsily increase until $S_a=S_b=0.5$ at the saturated field.

The physical picture for the above results could be understood as follows. For the $m=1/6$ plateau state at $J_1:J_2:J_3=1:2:2$, we note that if an approximate wave function defined by[13]

$$\psi_i=\frac{1}{\sqrt{6}}(2|\uparrow_{3i-2}\uparrow_{3i-1}\downarrow_{3i}\rangle\pm|\uparrow_{3i-2}\downarrow_{3i-1}\uparrow_{3i}\rangle\pm|\downarrow_{3i-2}\uparrow_{3i-1}\uparrow_{3i}\rangle)$$

$$(i=1,\ldots,L/3), \tag{2}$$

where $\uparrow_j$ ($\downarrow_j$) denotes spin up (down) on site j, is applied, one may obtain $\langle\psi_i|S_{3i-2}^z|\psi_i\rangle=1/3$, $\langle\psi_i|S_{3i-1}^z|\psi_i\rangle=1/3$, and $\langle\psi_i|S_{3i}^z|\psi_i\rangle=-1/6$, giving rise to a sequence $\{\ldots,(\frac{1}{3},\frac{1}{3},-\frac{1}{6}),\ldots\}$, and $m=(\frac{1}{3}+\frac{1}{3}-\frac{1}{6})/3=1/6$, which is in agreement with our DMRG results $\{\ldots,(0.345,0.345,-0.190),\ldots\}$. This observation shows that the ground state of this plateau state might be described by trimerized states.

Let H_{c_1} and H_{c_2} be the lower and upper critical magnetic fields at which the magnetization plateau appears and is destroyed, respectively. For $H_{c_1}\leqslant H\leqslant H_{c_2}$, the magnetization $m=m_p=1/6$; namely, the system falls into the magnetization plateau state. For $0\leqslant H\leqslant H_{c_1}$ and $J_1:J_2:J_3=1:2:2$, the magnetization curve shows the following behavior:

$$m(H)=m_p\left(\frac{H}{H_{c_1}}\right)\left[1+\alpha_1\left(1-\frac{H}{H_{c_1}}\right)-\alpha_2\left(1-\frac{H}{H_{c_1}}\right)^{2/3}\right], \tag{3}$$

where $H_{c_1}/J_1=1.44$, and the parameters $\alpha_1=2/3$ and $\alpha_2=1$. Obviously, when $H=0$ and $m=0$; $H=H_{c_1}$ and $m=m_p$. A fair comparison of Eq. (3) to the DMRG results is presented in Fig. 3(a). For $H_{c_2}\leqslant H\leqslant H_s$ and $J_1:J_2:J_3=1:2:2$, where H_s is the saturated magnetic field, the magnetization curve has the form of

$$m(H)=m_p+(H-H_{c_2})\left\{k_c+(H_s-H)\left[\frac{\beta_1}{(H-H_{c_2})^{1/3}}-\frac{\beta_2}{(H_s-H)^{1/3}}\right]\right\}, \tag{4}$$

where $k_c=(m_s-m_p)/(H_s-H_{c_2})$, with m_s being the saturation magnetization, and β_1 and β_2 the parameters. One may see that when $H=H_{c_2}$, $m=m_p$, and when $H=H_s$, $m=m_s$. A nice fitting to the DMRG result gives the parameters $H_{c_2}/J_1=3.15$, $m_s=1/2$, $H_s/J_1=4.55$, $\beta_1=0.143$, $\beta_2=0.178$, and $k_c=0.238$, as shown in Fig. 3(b). It should be remarked that from the phenomenological Eqs. (3) and (4), we find that, away from the plateau region, the magnetic-field dependence of the magnetization of this model differs from those of Haldane-type spin chains where $m(H)\sim(H-H_{c_1})^{1/2}$.

To explore further the magnetic properties of the frustrated spin-1/2 Heisenberg diamond chain in the ground states with the couplings $J_1:J_2:J_3=1:2:2$ at different external fields, let us look at the static structure factor $S(q)$ which is defined as

$$S(q)=\sum_j e^{iqj}\langle S_j^z S_0^z\rangle, \tag{5}$$

where q is the wave vector and $\langle S_j^z S_0^z\rangle$ is the spin-correlation function in the ground state. As demonstrated in Fig. 4(a), in the absence of the external field, $S(q)$ shows three peaks: two at $q=\pi/3$ and $5\pi/3$, and one at $q=\pi$, which are quite dif-

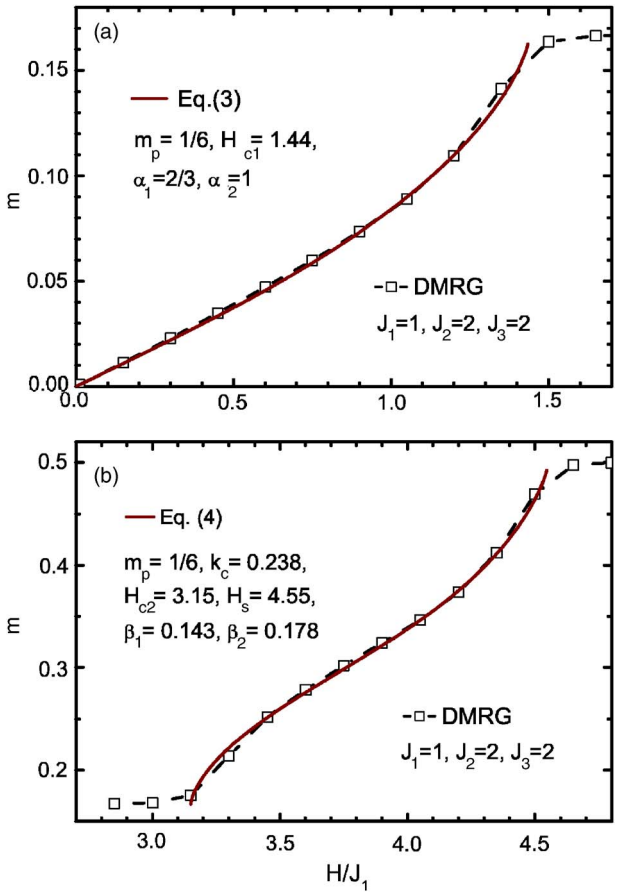

FIG. 3. (Color online) For a spin-1/2 frustrated Heisenberg diamond chain with fixed couplings $J_1:J_2:J_3=1:2:2$, the DMRG results of the magnetization per site m as a function of magnetic field H away from the plateau state can be fairly fitted by Eqs. (3) and (4) for (a) $0 \leqslant H \leqslant H_{c_1}$ and (b) $H_{c_2} \leqslant H \leqslant H_s$.

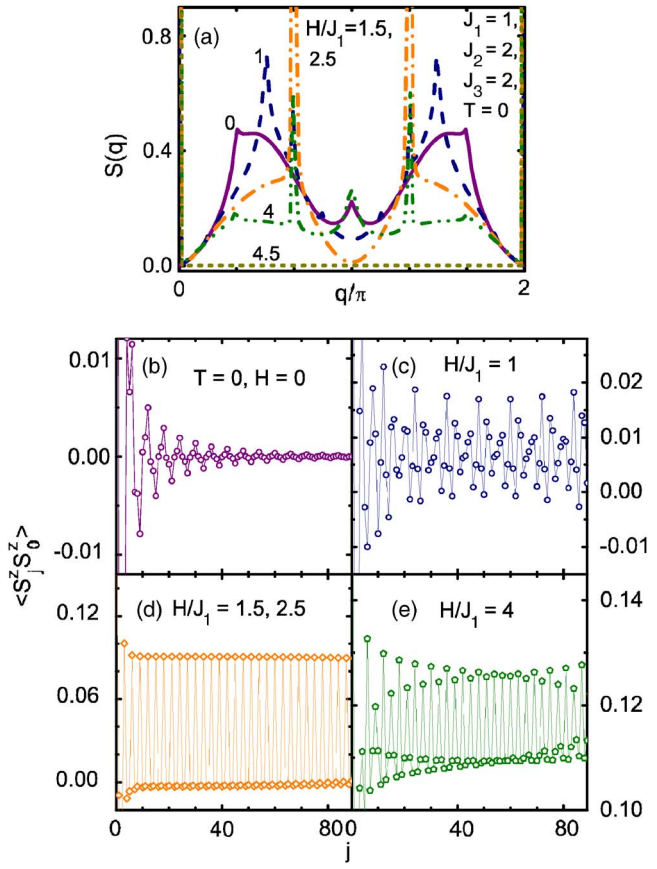

FIG. 4. (Color online) For a spin-1/2 frustrated Heisenberg diamond chain with fixed couplings $J_1:J_2:J_3=1:2:2$, (a) the static structure factor $S(q)$ in the ground states under different external fields and the spatial dependence of the spin-correlation function $\langle S_j^z S_0^z \rangle$ in the ground states under external fields (b) $H/J_1=0$, (c) 1, (d) 1.5 and 2.5, and (e) 4.

ferent from those of the spin $S=1/2$ Heisenberg AF chain, where $S(q)$ only diverges at $q=\pi$. As indicated by Eq. (5), the peaks of $S(q)$ reflect the periods of the spin-correlation function $\langle S_j^z S_0^z \rangle$; i.e., the peaks at $q=\pi/3$ $(5\pi/3)$ and π reflect the periods of 6 and 2 for $\langle S_j^z S_0^z \rangle$, respectively. As shown in Fig. 4(b), in the absence of the external field, $\langle S_j^z S_0^z \rangle$ changes sign every three sites, which really corresponds to the periods of 6 and 2. With the increasing magnetic field, the small peak of $S(q)$ at $q=\pi$ becomes a round valley while the peak at $q=\pi/3$ $(5\pi/3)$ continuously shifts toward $q=2\pi/3$ $(4\pi/3)$ with the height enhanced, indicating the corruption of the periods of 6 and 2 but the emergence of the new period $\in(3,6)$ for $\langle S_j^z S_0^z \rangle$, as shown in Fig. 4(c). At the field $H/J_1=1.5$, two peaks shift to $q=2\pi/3$ and $4\pi/3$ and merge into the peaks already existing there, showing the existence of period 3 for $\langle S_j^z S_0^z \rangle$, as clearly displayed in Fig. 4(d). The valley and peaks of $S(q)$ are kept intact in the plateau state at $m=1/6$. When the plateau state is destroyed at the field $H/J_1=4$, the peaks at $q=2\pi/3$ and $4\pi/3$ are depressed dramatically while the peaks at $q=\pi/3$, $5\pi/3$, and π appear again with very small heights, revealing the absence of period 3 and the slight presence of periods 2 and 6, as shown in Fig. 4(e). At the field $H/J_1=4.8$, all peaks disappear and become zero, except for the peak at $q=0$, which is the saturated state. Therefore, the static structure factor $S(q)$ shows different characteristics in different magnetic fields.[18] On the other hand, it is known that $S(q)$ also reflects the low-lying excitations of the system. It is thus reasonable to expect that the low-lying excitations of the frustrated diamond chain will behave differently in different magnetic fields.

To investigate the zero-field static structure factor $S(q)$ in the ground state for the frustrated spin-1/2 diamond chains with various AF couplings, the four cases with $J_1=1$, $J_3>0$, and $J_2=0.5$, 1, 2, and 4, are shown in Figs. 5(a)–5(d), respectively. For $J_2=0.5$, as shown in Fig. 5(a), $S(q)$ displays a sharp peak at $q=\pi$ when $J_3<0.5$, and three peaks at $q=0$, $2\pi/3$, and $4\pi/3$ when $J_3>0.5$. It is shown from the ground-state phase diagram[10] that the system is in the spin fluid (SF) phase when $J_1=1$, $J_2=0.5$, and $J_3<0.5$, and enters into the ferrimagnetic phase when $J_1=1$, $J_2=0.5$, and $J_3>0.5$. For $J_2=1$, as indicated in Fig. 5(b), the incommensurate peaks exist, such as the case of $J_3=0.8$, where the system is in the dimerized (D) phase.[10] For $J_2=2$, as manifested in Fig. 5(c), $S(q)$ has a sharp peak at $q=\pi$ and two ignorable peaks at $\pi/3$ and $5\pi/3$ when $J_3<1$; three sharp peaks at $q=0$, $2\pi/3$,

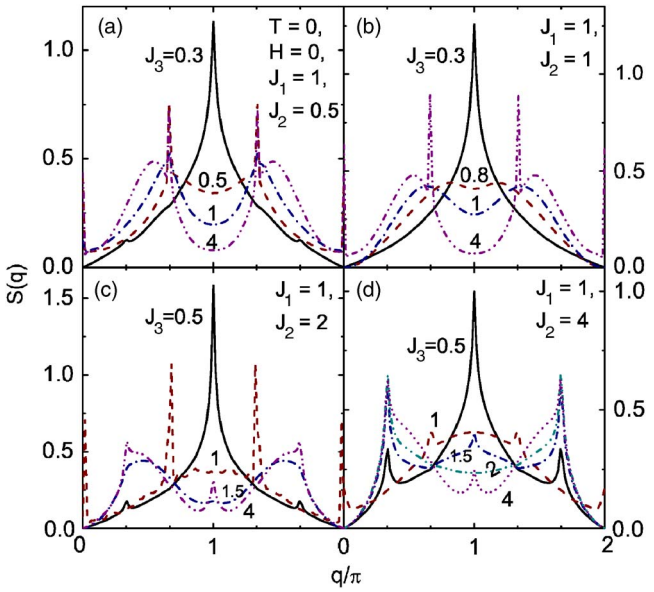

FIG. 5. (Color online) Zero-field static structure factor $S(q)$ in the ground states for the spin-1/2 frustrated Heisenberg diamond chains with length $L=120$, $J_1=1$, $J_3>0$, and J_2 taken to be (a) 0.5, (b) 1, (c) 2, and (d) 4.

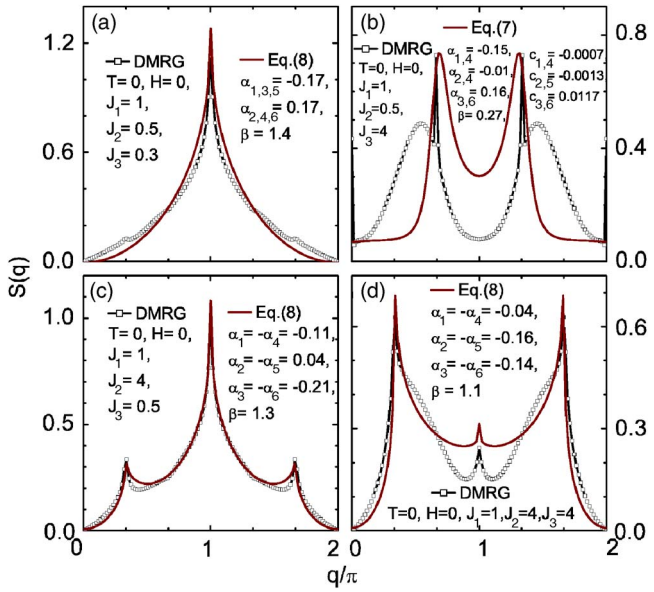

FIG. 6. (Color online) DMRG results of the zero-field static structure factor as a function of wave vector for the spin-1/2 frustrated Heisenberg diamond chains are fitted: (a) $J_1=1$, $J_2=0.5$, and $J_3=0.3$ by Eq. (8); (b) $J_1=1$, $J_2=0.5$, and $J_3=4$ by Eq. (7); (c) $J_1=1$, $J_2=4$, and $J_3=0.5$; and (d) $J_1=1$, $J_2=4$, and $J_3=4$ by Eq. (8).

and $4\pi/3$ when $J_3=1$; a round valley ($J_3=1.5$) or a small peak ($J_3=4$) at $q=\pi$; and two mediate peaks at $\pi/3$ and $5\pi/3$ when $J_3>1$. The system with $J_1=1$ and $J_2=2$ is in the D phase when $1<J_3<2.8$, and in the SF phase when $J_3<1$ or $J_3>2.8$.[10] For $J_2=4$ revealed in Fig. 5(d), the situations are similar to that of Fig. 5(c), but here only the SF phase exists for the system with $J_1=1$, $J_2=4$, and $J_3>0$.[10] It turns out that even in the same phase, such as the SF phase, the zero-field static structure factor $S(q)$ could display different characteristics for different AF couplings. In fact, we note that the exotic peak of $S(q)$ has been experimentally observed in the diamond-type compound $Sr_3Cu_3(PO_4)_4$.[19]

If the spin-correlation function for the spin-S chain can be expressed as $\langle S_j^z S_0^z\rangle=\alpha(-1)^j e^{-j\beta}$, where α and β are two parameters, its static structure factor will take the form of

$$S(q)=\frac{S(S+1)}{3}-\frac{\alpha(\cos q+e^{-\beta})}{\cos q+\cosh\beta}, \tag{6}$$

which can recover exactly the $S(q)$ of the spin-S AKLT chain $S(q)=\frac{S+1}{3}\frac{1-\cos q}{1+\cos q+2/S(S+2)}$ (Ref. 20), with $\alpha=(S+1)^2/3$ and $\beta=\ln(1+2/S)$. Equation (6) has a peak at wave vector $q=\pi$. By noting that the zero-field static structure factor $S(q)$ for the frustrated diamond chains displays peaks at wave vectors $q=a\pi/3$ $(a=0,1,2,3,4,5)$ for different AF couplings, the spin-correlation function $\langle S_j^z S_0^z\rangle$ could be reasonably divided into six modes $\langle S_{6m+l}^z S_0^z\rangle=c_l+\alpha_l e^{-(6m+l)\beta}$ or $\langle S_{6m+l}^z S_0^z\rangle=\alpha_l(6m+l)^{-\beta}$ with $j=6m+l$ and $l=1,2,\ldots,6$, whose contributions to the static structure factor should be considered separately.[21] Thus, the static structure factor for the present systems could be mimicked by a superposition of six modes, which leads to

$$S(q)=\sum_{l=1}^{6}\left\{\alpha_l\frac{e^{(6-l)\beta}\cos(lq)-e^{-l\beta}\cos[(6-l)q]}{\cosh(6\beta)-\cos(6q)}+c_l\frac{\cos(lq)-\cos[(6-l)q]}{1-\cos(6q)}\right\}+\frac{1}{4} \tag{7}$$

or

$$S(q)=\sum_{l=1}^{6}\alpha_l\sum_{m=0}^{\infty}2(6m+l)^{-\beta}\cos[(6m+1)q]+\frac{1}{4}, \tag{8}$$

respectively, depending on which phase the system falls into, where α_l, c_l, and β are coupling-dependent parameters.

As presented in Fig. 6, the DMRG results of the static structure factor as a function of wave vector are fitted by Eqs. (7) and (8) for the spin-1/2 frustrated Heisenberg diamond chains with various AF couplings in zero magnetic field. It can be found that the characteristic peaks can be well fitted by Eqs. (7) and (8), with only a slightly quantitative deviation, showing that the main features of the static structure factor for the present systems can be reproduced by a linear superposition of six modes. The fitting results give six different modes in general, as shown in Fig. 4(b).

To further understand the above-mentioned behaviors of the zero-field static structure factor $S(q)$, we have applied the Jordan-Wigner (JW) transformation to study the low-lying excitations of the spin-1/2 frustrated Heisenberg diamond chain with various AF couplings (see the Appendix for derivations). It can be seen that the zero-field low-lying fermionic excitation $\varepsilon(k)$ behaves differently for different AF couplings, as shown in Figs. 7(a)–7(d). Obviously, these low-lying excitations are responsible for the DMRG calculated behaviors of $S(q)$, where the positions of minima of $\varepsilon(k)$ for

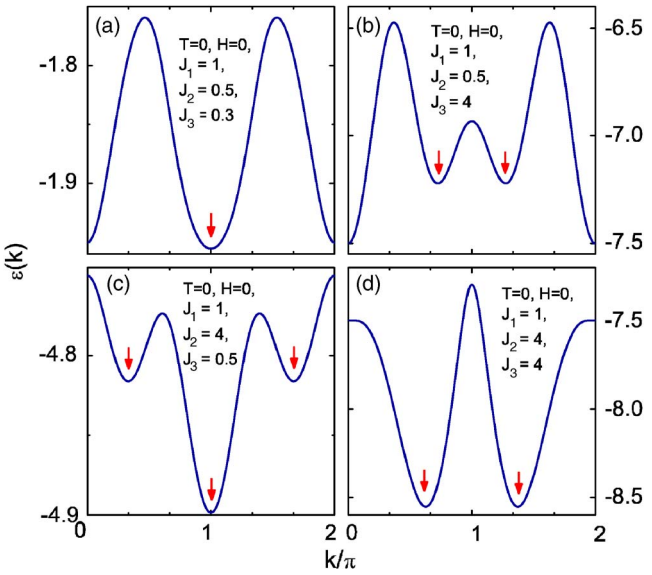

FIG. 7. (Color online) Zero-field low-lying fermionic excitation as a function of wave vector for the spin-1/2 frustrated Heisenberg diamond chain with (a) $J_1=1$, $J_2=0.5$, and $J_3=0.3$; (b) $J_1=1$, $J_2=0.5$, and $J_3=4$; (c) $J_1=1$, $J_2=4$, and $J_3=0.5$; and (d) $J_1=1$, $J_2=4$, $J_3=4$. The arrows indicate the locations of minima of $\varepsilon(k)$.

different AF couplings, as indicated by arrows in Figs. 7(a)–7(c), are exactly consistent with the locations of the peaks of the zero-field static structure factor $S(q)$ shown in Figs. 6(a)–6(c), respectively, although there is somewhat a deviation between Figs. 7(d) and 6(d). It also shows that the six modes suggested by Eqs. (7) and (8) are closely related to the low-lying excitations of the system.

B. Magnetization, susceptibility, and specific heat

The magnetization process for the spin-1/2 frustrated diamond chain with $J_1=1$, $J_3>0$, and $J_2=0.5$ and 2 is shown in Figs. 8(a) and 8(b), where temperature is fixed as $T/J_1=0.05$. It is found that the magnetization exhibits different behaviors for different AF couplings: a plateau at $m=1/6$ is observed, in agreement with the ground-state phase diagram;[12,13] for $J_2=0.5$, as shown in Fig. 8(a), the larger J_3 is, the larger the width of the plateau at $m=1/6$ becomes; for $J_2=2$, as presented in Fig. 8(b), the width of the plateau at $m=1/6$ becomes larger with increasing $J_3<1$ and then turns smaller with increasing $J_3>1$; for $J_3<1$, the larger J_2 is, the larger is the width of the plateau at $m=1/6$; for $J_3=2$, the larger J_2 is, the smaller is the width of the plateau at $m=1/6$. The saturated field is obviously promoted with increasing AF J_3 and J_2.

Figures 8(c) and 8(d) give the susceptibility χ as a function of temperature T for the spin-1/2 frustrated diamond chain with $J_1=1$, $J_3>0$, and $J_2=0.5$ and 2, while the external field is taken as $H/J_1=0.01$. For $J_2=0.5$, as shown in Fig. 8(c), the low-temperature part of $\chi(T)$ remains finite when $J_3<0.5$ and becomes divergent when $J_3>0.5$. As clearly manifested in the inset of Fig. 8(c), $J_3=0.5$ is the critical value which is consistent with the behaviors of the static structure factor $S(q)$ in Fig. 5(a). For $J_2=2$, as shown in Fig.

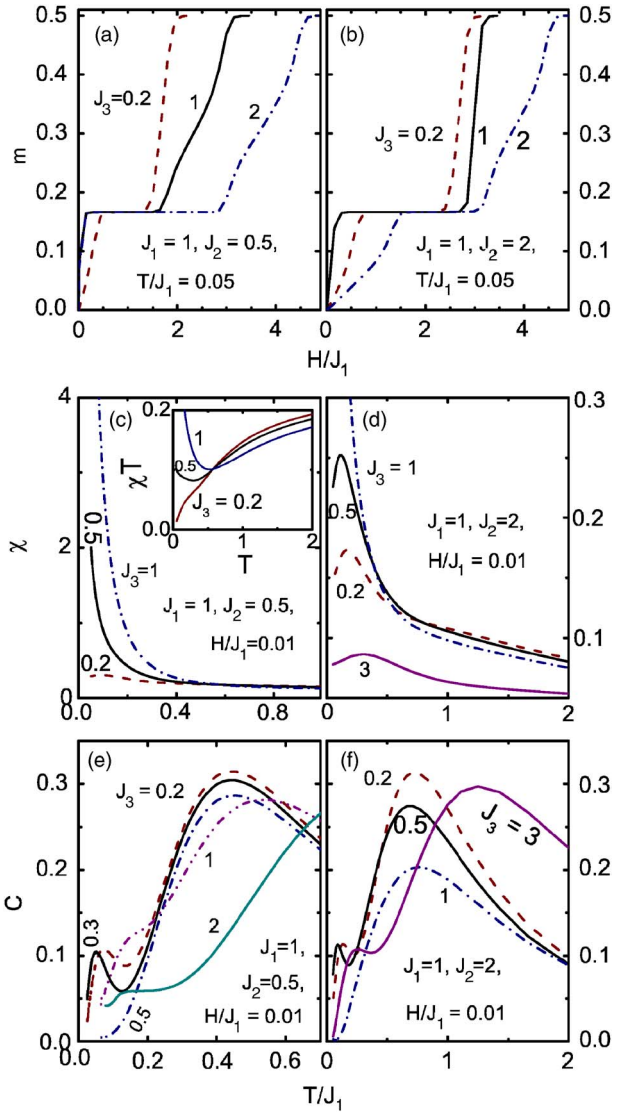

FIG. 8. (Color online) For the spin-1/2 frustrated Heisenberg diamond chains with $J_1=1$ and $J_3>0$, the magnetization process $m(H)$ at temperature $T/J_1=0.05$ with (a) $J_2=0.5$ and (b) $J_2=2$; the susceptibility $\chi(T)$ at field $H/J_1=0.01$ with (c) $J_2=0.5$ and (d) $J_2=2$; the specific heat $C(T)$ at field $H/J_1=0.01$ with (e) $J_2=0.5$ and (f) $J_2=2$.

8(d), an unobvious double-peak structure at low temperature is observed at small and large J_3 such as 0.2 and 3. The temperature dependence of the specific heat C with $J_1=1$, $J_3>0$, and $J_2=0.5$ and 2 is shown in Figs. 8(e) and 8(f), while the external field is fixed at $H/J_1=0.01$. For $J_2=0.5$, as given in Fig. 8(e), a double-peak structure of $C(T)$ is observed at low temperatures for small and large J_3 such as 0.3 and 1. The case with $J_2=2$ shown in Fig. 8(f) exhibits similar characteristics. Thus, the thermodynamics of the system demonstrate different behaviors for different AF couplings. As manifested in Fig. 5, the low-lying excitations behave differently for different AF couplings. The double-peak structure of the susceptibility as well as the specific heat could be attributed to the excited gaps in the low-lying excitation spectrum.[22]

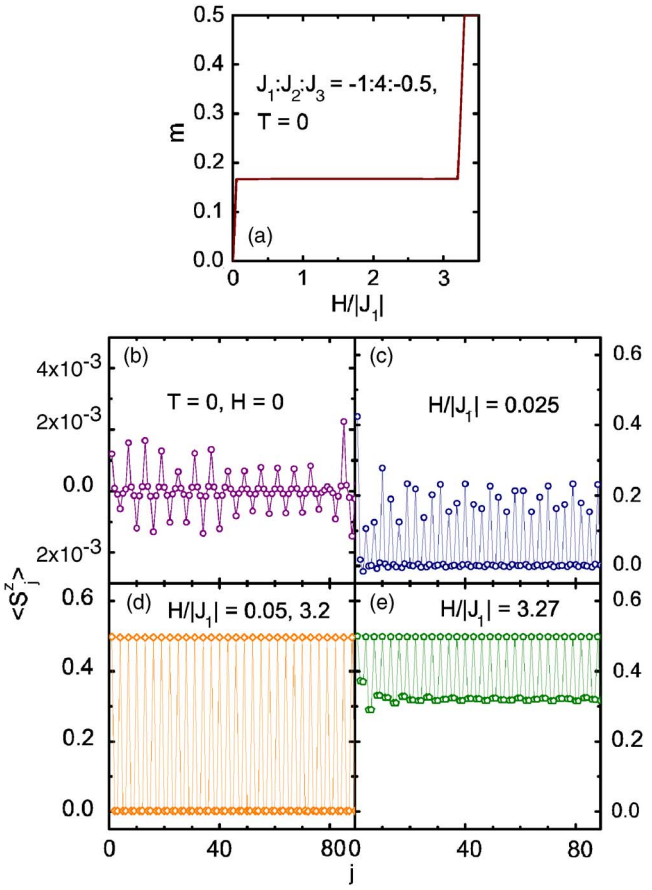

FIG. 9. (Color online) For a spin-1/2 frustrated Heisenberg diamond chain with fixed couplings $J_1:J_2:J_3=-1:4:-0.5$, (a) the magnetization per site m as a function of magnetic field H in the ground states; and the spatial dependence of the averaged local magnetic moment $\langle S_j^z \rangle$ in the ground states with external field (b) $H/|J_1|=0$, (c) 0.025, (d) 0.05 and 3.2, and (e) 3.27.

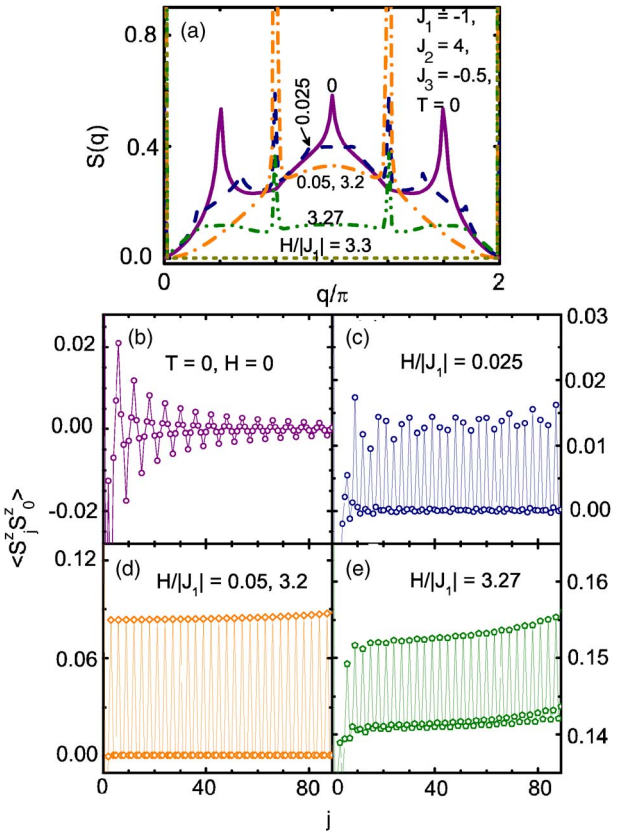

FIG. 10. (Color online) For a spin-1/2 frustrated Heisenberg diamond chain with fixed couplings $J_1:J_2:J_3=-1:4:-0.5$, (a) the static structure factor $S(q)$ in the ground states with different external fields and the spatial dependence of the spin-correlation function $\langle S_j^z S_0^z \rangle$ in the ground states with external field (b) $H/|J_1|=0$, (c) 0.025, (d) 0.05 and 3.2, and (e) 3.27.

IV. A FRUSTRATED DIAMOND CHAIN WITH COMPETING INTERACTIONS ($J_1, J_3 < 0, J_2 > 0$)

A. Local magnetic moment and spin-correlation function

Figure 9(a) shows the magnetization process of a frustrated spin-1/2 Heisenberg diamond chain in the ground states with the couplings $J_1:J_2:J_3=-1:4:-0.5$. The plateau of magnetization per site $m=1/6$ is clearly obtained. To understand the occurrence of the magnetization plateau, the spatial dependence of the averaged local magnetic moment $\langle S_j^z \rangle$ in the ground states at different external fields is calculated. It is seen that in the absence of the magnetic field, as presented in Fig. 9(b), the expectation values of $\langle S_j^z \rangle$ change sign every three sites within a very small range of $(-2 \times 10^{-4}, 2 \times 10^{-4})$, resulting in the magnetization per site $m=0$. With the increasing field, the expectation values of $\langle S_j^z \rangle$ increase, whose unit of three spins is gradually divided into a pair and a single, as displayed in Fig. 9(c). At the field $H/|J_1|=0.05$, as illustrated in Fig. 9(d), the behavior of $\langle S_j^z \rangle$ shows a perfect sequence such as $\{\ldots,(S_a,S_b,S_b),\ldots\}$ with $S_a=0.496$ and $S_b=0.002$, giving rise to the magnetization per site $m=1/6$. In addition, the sequence is fixed with the increasing field until $H/|J_1|=3.2$, corresponding to the plateau of $m=1/6$. As the field is enhanced further, the double S_b begin to rise, and the sequence becomes a waved series with a smaller swing of (S_a-S_b), as revealed in Fig. 9(e), which corresponds to the plateau state at $m=1/6$ that is destroyed. It is noted that the increase of m is mainly attributed to the promotion of double S_b, as S_a is already saturated until $S_a=S_b=0.5$ at the saturated field.

As discussed above, the physical picture of the $m=1/6$ plateau state at $J_1:J_2:J_3=-1:4:-0.5$ can be understood by the following approximate wave function:

$$\psi_i = \frac{1}{\sqrt{2}}(|\uparrow_{3i-2}\uparrow_{3i-1}\downarrow_{3i}\rangle \pm |\uparrow_{3i-2}\downarrow_{3i-1}\uparrow_{3i}\rangle).$$

By use of this wave function, we have $\langle \psi_i | S_{3i-2}^z | \psi_i \rangle = 1/2$, $\langle \psi_i | S_{3i-1}^z | \psi_i \rangle = 0$, and $\langle \psi_i | S_{3i}^z | \psi_i \rangle = 0$, leading to a sequence of $\{\ldots,(1/2,0,0),\ldots\}$, and $m=(1/2+0+0)/3=1/6$. This is in agreement with our DMRG results $\{\ldots, (0.496, 0.002, 0.002),\ldots\}$.

The static structure factor $S(q)$ of the frustrated spin-1/2 Heisenberg diamond chain with the competing couplings $J_1:J_2:J_3=-1:4:-0.5$ in the ground states is considered in different external fields. At zero field, shown in Fig. 10(a),

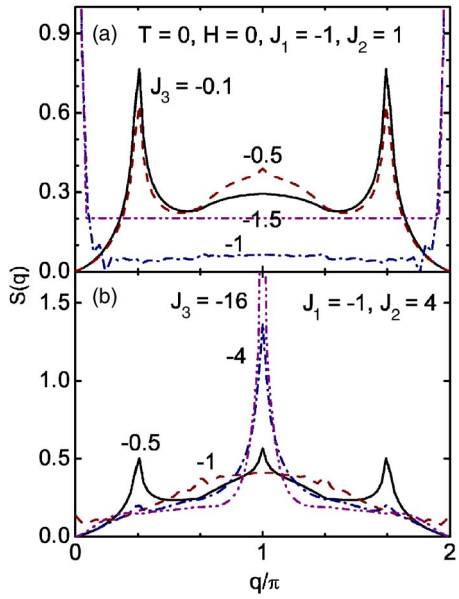

FIG. 11. (Color online) Zero-field static structure factor $S(q)$ in the ground states for the spin-1/2 frustrated Heisengberg diamond chains with length $L=120$, $J_1=-1$, $J_3<0$, and J_2 taken as (a) 1 and (b) 4.

$S(q)$ has three peaks at $q=\pi/3$, $5\pi/3$, and π with mediate heights, which reflects the periods of 6 and 2 for $\langle S_j^z S_0^z\rangle$, respectively. As shown in Fig. 10(b), in the absence of the external field, $\langle S_j^z S_0^z\rangle$ changes sign every three sites, corresponding to the periods of 6 and 2. With the increasing field, the peak at $q=\pi$ becomes flat with height depressed forwardly, while the peak at $q=\pi/3$ ($5\pi/3$) is divided into two peaks shifting oppositely from $q=\pi/3$ ($5\pi/3$) with height decreased, indicating the corruption of the periods of 6 and 2 and the emergence of new periods for $\langle S_j^z S_0^z\rangle$, as shown in Fig. 10(c). At the field $H/|J_1|=0.05$, two shifting peaks have reached $q=2\pi/3$ and $4\pi/3$, and are merged with the existing peaks, showing the occurrence of period 3 for $\langle S_j^z S_0^z\rangle$, as clearly displayed in Fig. 10(d). The flat and peaks remain constant during the plateau state at $m=1/6$. When the plateau state is destroyed at field $H/J_1=3.27$, the peaks at $q=2\pi/3$ and $4\pi/3$ are depressed sharply, revealing the decay of period 3, as shown in Fig. 10(e). At the saturated field of $H/J_1=3.3$, all peaks disappear and become flat with the value zero, which is the saturated state. So, the static structure factor $S(q)$ shows different characteristics in different magnetic fields. Similar to the discussions in Fig. 4, the low-lying excitations of this frustrated diamond chain would also behave differently in different magnetic fields.

To further investigate the zero-field static structure factor $S(q)$ in the ground state for the frustrated spin-1/2 diamond chains with various J_1, $J_3<0$, and $J_2>0$, two cases with $J_1=-1$, $J_3<0$, and $J_2=1$ and 4 are illustrated in Figs. 11(a) and 11(b). For $J_2=1$, $S(q)$ shows a round peak at $q=\pi$, two sharp peaks at $\pi/3$ and $5\pi/3$ when $|J_3|<1$, and a very sharp peak at $q=0$ when $|J_3|>1$. For $J_2=4$, $S(q)$ shows three peaks at $q=\pi/3$, π, and $5\pi/3$ as $|J_3|<1$, and a very sharp peak at $q=\pi$ and nearly ignorable peaks at $\pi/3$ and $5\pi/3$ as $|J_3|>1$. In general, the zero-field static structure factor $S(q)$ shows different characteristics with different competing couplings, whose exotic characteristics could be experimentally observed in the related diamond-type compounds.

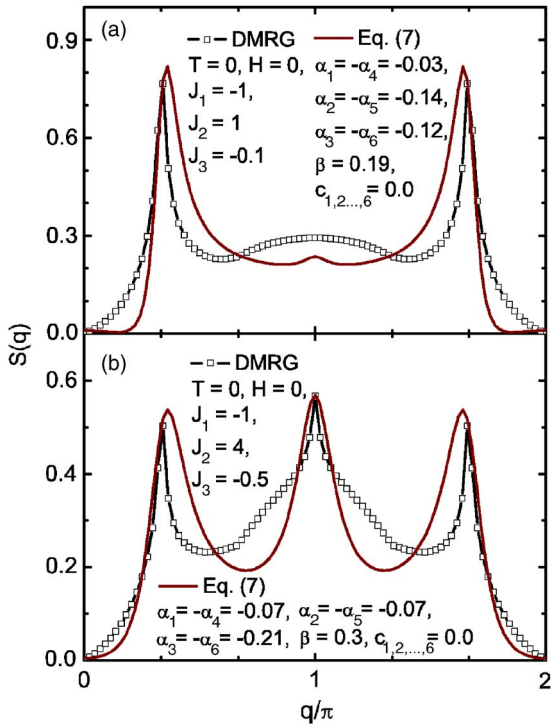

FIG. 12. (Color online) DMRG results of the zero-field static structure factor as a function of wave vector are fitted by Eq. (7) for the spin-1/2 frustrated Heisenberg diamond chains with (a) $J_1=-1$, $J_2=1$, and $J_3=-0.1$ and (b) $J_1=-1$, $J_2=4$, and $J_3=-0.5$.

As shown in Fig. 12, the DMRG results of the static structure factor as a function of wave vector are fitted by Eq. (7) for the spin-1/2 frustrated Heisenberg diamond chains with J_1, $J_3<0$, and $J_2>0$. It can be found that the characteristic behaviors can be nicely fitted by Eq. (7), with only a slightly quantitative deviation, showing that the main features of the static structure factor for the present systems can be captured by a superposition of six modes. It is consistent with the fact that the spin-correlation function for the present systems has six different modes, as manifested in Fig. 10(b).

Similar to case (a) with all AF couplings in the last section, the characteristics of zero-field $S(q)$ for the spin-1/2 frustrated Heisenberg diamond chain with J_1, $J_3<0$, and $J_2>0$ can be further undersood in terms of the low-lying excitations of the system (see Appendix A). By means of the JW transformation, the zero-field low-lying fermionic excitation $\varepsilon(k)$ of the present case is calculated, as shown in Figs. 13(a) and 13(b). It is found that the zero-field low-lying fermionic excitation $\varepsilon(k)$ differs for different couplings, but the positions of minima of $\varepsilon(k)$ for different couplings, as indicated by arrows in Figs. 13(a) and 13(b), appear to be the same. One may see that these positions coincide exactly with the locations of peaks of the zero-field static structure factor $S(q)$ manifested in Figs. 12(a) and 12(b), respectively, showing that our fitting equation is qualitatively consistent with the low-lying excitations of the system.

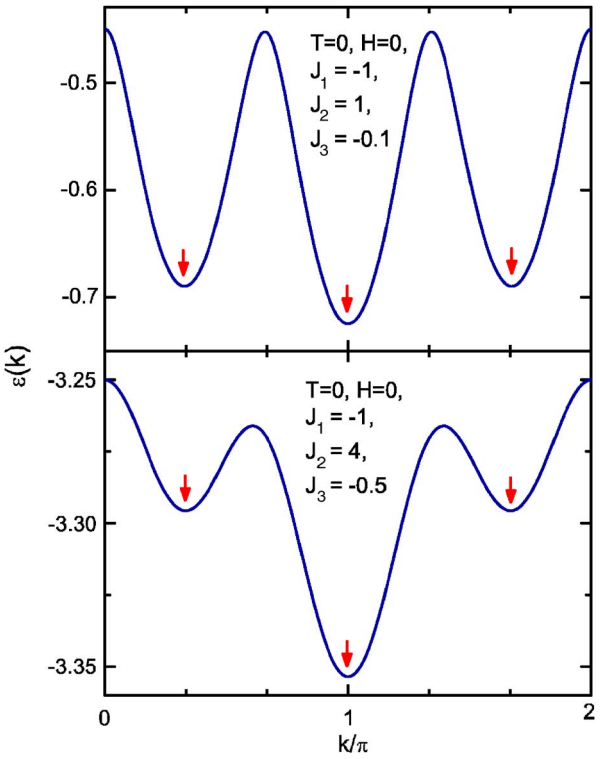

FIG. 13. (Color online) Zero-field low-lying fermionic excitation as a function of wave vector for the spin-1/2 frustrated Heisenberg diamond chain with (a) $J_1=-1$, $J_2=1$, and $J_3=-0.1$ and (b) $J_1=-1$, $J_2=4$, and $J_3=-0.5$. The arrows indicate the locations of minima of $\varepsilon(k)$.

B. Magnetization, susceptibility, and specific heat

Figures 14(a) and 14(b) show the magnetization process for the spin-1/2 frustrated diamond chain at a finite temperature $T/|J_1|=0.05$ with $J_1=-1$, $J_3<0$, and $J_2=1$ and 4. It is shown that the magnetization exhibits different behaviors for different J_1, $J_3<0$, and $J_2>0$. A plateau at $m=1/6$ is observed at small $|J_3|$. With a fixed J_2, the larger $|J_3|$ is, the smaller is the width of the plateau at $m=1/6$, and the plateau disappears when $|J_3|$ exceeds the critical value; for a fixed J_3, the larger J_2 is, the wider is the width of the plateau at $m=1/6$; the saturation field is obviously depressed with the increase of $|J_3|$ at a fixed J_2, and is enhanced with the increase of J_2 at a fixed J_3.

Figures 14(c) and 14(d) manifest the susceptibility χ as a function of temperature T for the spin-1/2 frustrated diamond chain with $J_1=-1$, $J_3<0$, and $J_2=1$ and 4, respectively, where the external field is taken as $H/|J_1|=0.01$. For $J_2=1$, the low-temperature part of $\chi(T)$ remains finite when $|J_3|<1$ and becomes divergent when $|J_3|>1$. As clearly revealed in the inset of Fig. 14(c), $J_3=-1$ is the critical value, which is in agreement with the behaviors of the static structure factor $S(q)$ shown in Fig. 11(a). For $J_2=4$, a clear double-peak structure of $\chi(T)$ is obtained at $|J_3|=8$. The temperature dependence of the specific heat C with $J_1=-1$, $J_3<0$, and $J_2=1$ and 4 is shown in Figs. 14(e) and 14(f), where the external field is fixed as $H/|J_1|=0.01$. For $J_2=1$, a double-peak structure of $C(T)$ is observed for the case of $|J_3|=0.5$. The case with $J_2=4$ shown in Fig. 14(f) exhibits similar characteristics. It is also found that owing to the competitions among J_1, J_3, and J_2, the thermodynamics demonstrate rich behaviors at different couplings. As reflected in Fig. 11, the low-lying excitations behave differently with various F interactions J_1, J_3, and AF interaction J_2, while the excitation gaps could induce the double-peak structure in the susceptibility as well as in the specific heat.[22]

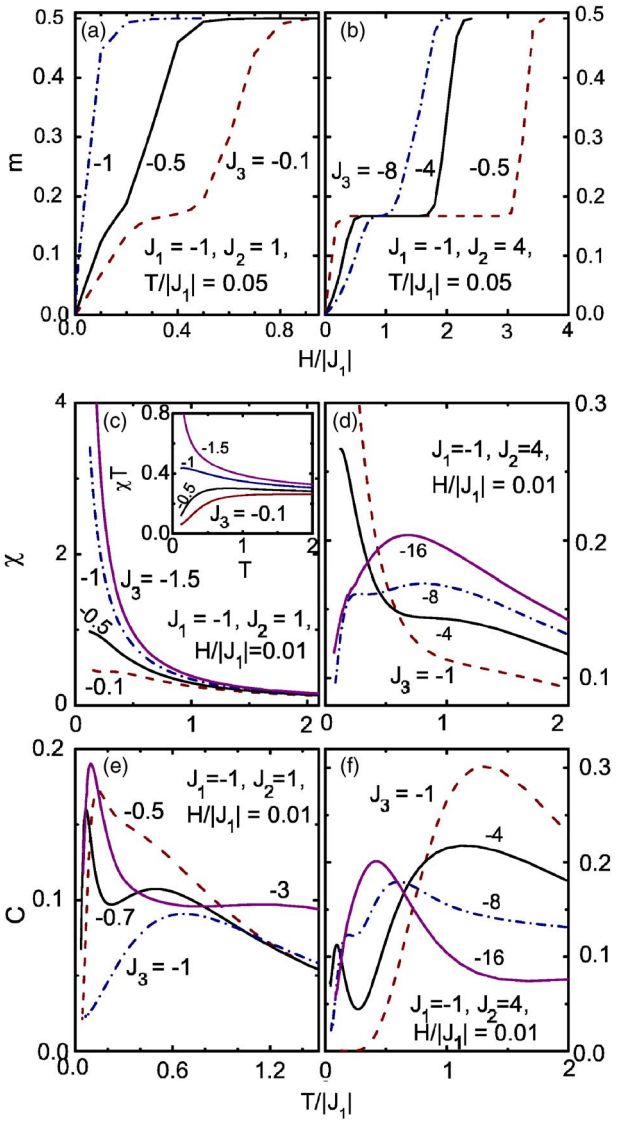

FIG. 14. (Color online) For the spin-1/2 frustrated Heisenberg diamond chains with $J_1=-1$ and $J_3<0$, the magnetization process $m(H)$ at temperature $T/J_1=0.05$ with (a) $J_2=1$ and (b) $J_2=4$; the susceptibility $\chi(T)$ at field $H/J_1=0.01$ with (c) $J_2=1$ and (d) $J_2=4$; the specific heat $C(T)$ at field $H/J_1=0.01$ with (e) $J_2=1$ and (f) $J_2=4$.

V. A DIAMOND CHAIN WITHOUT FRUSTRATION ($J_1, J_2>0, J_3<0$)

A. Local magnetic moment and spin-correlation function

Figure 15(a) shows the magnetization process of a nonfrustrated spin-1/2 Heisenberg diamond chain in the ground

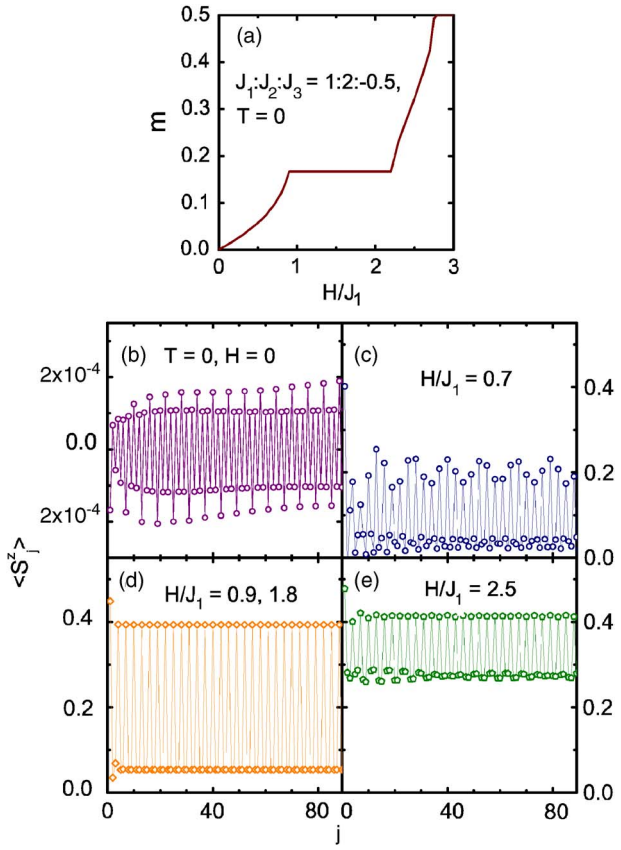

FIG. 15. (Color online) For a spin-1/2 nonfrustrated Heisenberg diamond chain with fixed couplings $J_1:J_2:J_3=1:2:-0.5$, (a) the magnetization per site m as a function of magnetic field H in the ground states and the spatial dependence of the averaged local magnetic moment $\langle S_j^z \rangle$ in the ground states with external fields (b) $H/J_1=0$, (c) 0.7, (d) 0.9 and 1.8, and (e) 2.5.

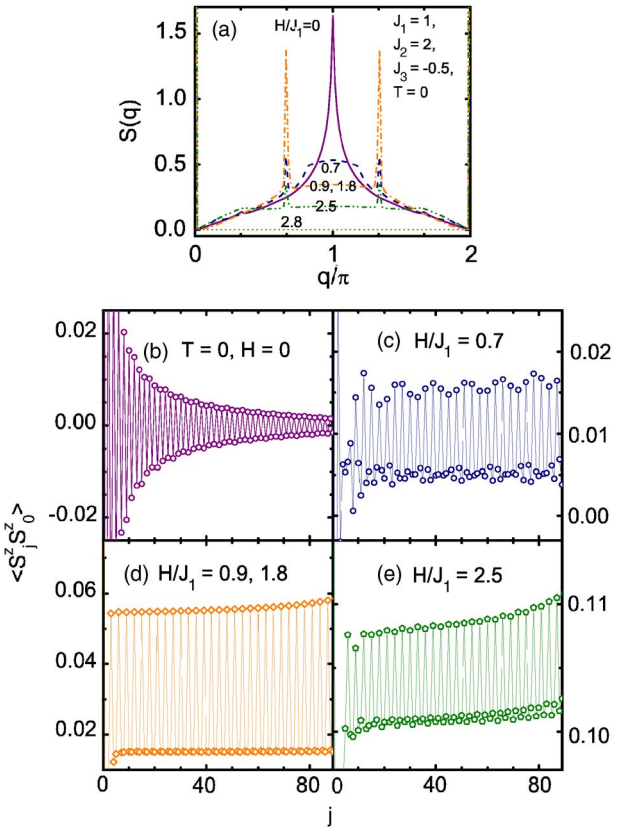

FIG. 16. (Color online) For a spin-1/2 nonfrustrated Heisenberg diamond chain with fixed couplings $J_1:J_2:J_3=1:2:-0.5$, (a) the static structure factor $S(q)$ in the ground states with different external fields and the spatial dependence of the spin-correlation function $\langle S_j^z S_0^z \rangle$ in the ground states with external field (b) $H/J_1=0$, (c) 0.7, (d) 0.9 and 1.8, and (e) 2.5.

states with the couplings satisfying $J_1:J_2:J_3=1:2:-0.5$. The plateau of magnetization per site $m=1/6$ is observed. The appearance of the magnetization plateau can be understood from the spatial dependence of the averaged local magnetic moment $\langle S_j^z \rangle$ in the ground states under different external fields. In the absence of the external field, the expectation values of $\langle S_j^z \rangle$ change sign every one site with a waved swing within a very small range of $(-2\times10^{-4}, 2\times10^{-4})$, giving rise to the magnetization per site $m=0$. Under a finite field, every three successive spins have gradually cooperated into a pair and a single, as shown in Fig. 15(c). At $H/J_1=0.9$, as given in Fig. 15(d), $\langle S_j^z \rangle$ shows a perfect sequence such as $\{\ldots,(S_a,S_b,S_b),\ldots\}$ with $S_a=0.393$ and $S_b=0.053$, resulting in the magnetization per site $m=1/6$. Moreover, the sequence is fixed with the field increased until $H/J_1=1.8$, corresponding to the plateau state of $m=1/6$. As the field is increased further, double S_b begin to increase, and the sequence becomes a waved succession with a smaller swing of (S_a-S_b), as manifested in Fig. 15(e), which corresponds to the fact that the plateau state at $m=1/6$ is destroyed. It is observed that the increase of m at first is mainly attributed to the speedy boost of double S_b, and later, S_a starts to increase weakly until $S_a=S_b=0.5$ at the saturated field.

For this nonfrustrated case with couplings $J_1:J_2:J_3=1:2:-0.5$, the obtained perfect sequence of $\{\ldots, (0.393, 0.053), 0.053),\ldots\}$ for the $m=1/6$ plateau state could be understood by the following approximate trimerized wave function:

$$\psi_i = \frac{1}{3}(2|\uparrow_{3i-2}\uparrow_{3i-1}\downarrow_{3i}\rangle \pm 2|\uparrow_{3i-2}\downarrow_{3i-1}\uparrow_{3i}\rangle \pm |\downarrow_{3i-2}\uparrow_{3i-1}\uparrow_{3i}\rangle). \tag{9}$$

According to this function, we find $\langle\psi_i|S^z_{3i-2}|\psi_i\rangle=7/18$, $\langle\psi_i|S^z_{3i-1}|\psi_i\rangle=1/18$, and $\langle\psi_i|S^z_{3i}|\psi_i\rangle=1/18$, giving rise to a sequence of $\{\ldots,(7/18,1/18,1/18),\ldots\}$. It turns out that $m=(7/18+1/18+1/18)/3=1/6$. This observation implies that the ground state of the plateau state can also be described by the trimerized states.

The static structure factor $S(q)$ of the nonfrustrated spin-1/2 Heisenberg diamond chain in the ground states with the couplings $J_1:J_2:J_3=1:2:-0.5$ is probed in different external fields. As shown in Fig. 16(a), in the absence of the external field, $S(q)$ shows a sharp peak at $q=\pi$, similar to the behaviors of the $S=1/2$ Heisenberg AF chain, which reflects the period of 2 for $\langle S_j^z S_0^z \rangle$. As displayed in Fig. 16(b), at zero external field, $\langle S_j^z S_0^z \rangle$ changes sign every one lattice site, corresponding to the period of 2. When the field is increased, the peak at $q=\pi$ becomes a flat with the height depressed

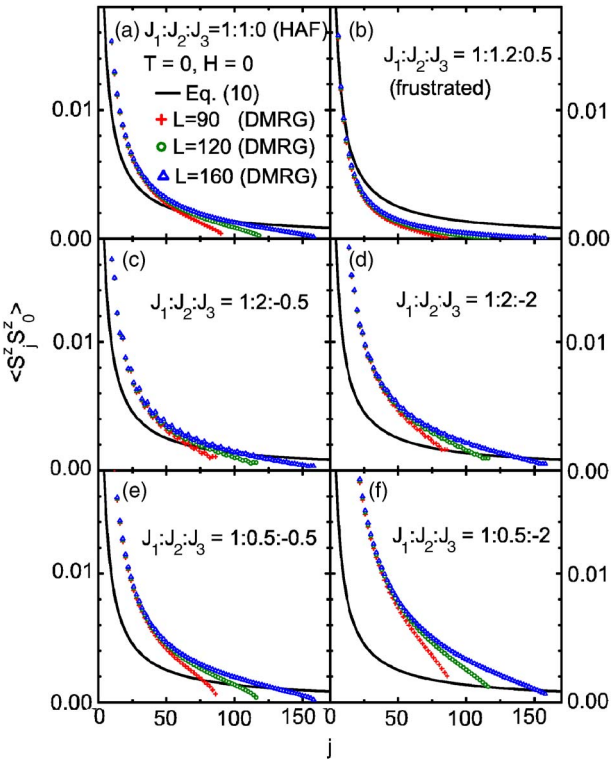

FIG. 17. (Color online) Zero-field static correlation function $\langle S_j^z S_0^z \rangle$ versus site j in the ground state for a spin-1/2 diamond chain with different lengths and various couplings. The coupling ratio $J_1:J_2:J_3$ is taken as (a) 1:1:0 (HAF), (b) 1:1.2:0.5 (frustrated), (c) $1:2:-0.5$, (d) $1:2:-2$, (e) $1:0.5:-0.5$, and (f) $1:0.5:-2$. The length is taken as $L=90$, 120, and 160.

greatly, while two new peaks with small heights at $q=2\pi/3$ and $4\pi/3$ appear, indicating the corruption of the period of 2 and the emergence of the new period of 3 for $\langle S_j^z S_0^z \rangle$, as demonstrated in Fig. 16(c). At the field $H/J_1=0.9$, the peaks at $q=0$, $2\pi/3$, and $4\pi/3$ become sharper. The flat and peaks of $S(q)$ remain unchanged during the plateau state at $m=1/6$. When the plateau state is destroyed at the field $H/J_1=2.5$, the peaks at $q=2\pi/3$ and $4\pi/3$ are suppressed dramatically, revealing the decay of period 3, as shown in Fig. 16(e). At the field $H/J_1=2.8$, all peaks disappear and become flat with the value zero, except for the peak at $q=0$, which is the saturated state. It can be stated that the static structure factor $S(q)$ shows various characteristics in different magnetic fields. Similar to what is discussed in Figs. 4 and 10, the low-lying excitations of this nonfrustrated diamond chain would also behave differently in different magnetic fields.

The zero-field static structure factor $S(q)$ in the ground state for the present system displays a peak at $q=\pi$ with different couplings, but whose static correlation function $\langle S_j^z S_0^z \rangle$ varies with the couplings. As illustrated in Fig. 17, only the values of $\langle S_j^z S_0^z \rangle$ are larger than zero presented for convenience. In order to gain deep insight into physics, for a comparison, we also include the static correlation function for the $S=1/2$ Heisenberg antiferromagnetic (HAF) chain in Fig. 17(a), whose asymptotic behavior has the form of[23,24]

$$\langle \mathbf{S}_j \cdot \mathbf{S}_0 \rangle \propto (-1)^j \frac{1}{(2\pi)^{3/2}} \frac{\sqrt{\ln j}}{j}. \tag{10}$$

Equation (10) is depicted as solid lines in Figs. 17. To take the finite-size effect into account, the length of the diamond chain is taken as $L=90$, 120, and 160, respectively. As revealed in Fig. 17(a), the DMRG result of the $S=1/2$ HAF chain with an infinite length agrees well with the solid line. Figure 17(b) shows that the static correlation function for the spin-1/2 diamond chain with frustrated couplings $J_1:J_2:J_3=1:1.2:0.5$ decays faster than that of the HAF chain. Compared with Figs. 17(c)–17(f), it can be found that all the static correlation functions for the spin-1/2 nonfrustrated diamond chain with AF interactions J_1 and J_2 and F interaction J_3 fall more slowly than that of the $S=1/2$ HAF chain; for fixed AF interactions J_1 and J_2, the static correlation functions drop more leisurely with the increasing F interaction $|J_3|$; for the fixed AF interaction J_1 and F interaction J_3, the static correlation functions decrease more rapidly with the increasing AF interaction J_2.

B. Magnetization, susceptibility, and specific heat

Figures 18(a) and 18(b) show the magnetization process for the spin-1/2 nonfrustrated diamond chain at a finite temperature $T/J_1=0.05$ with $J_1=1$, $J_3<0$, and $J_2=0.5$ and 2. It is found that the magnetization behaves differently with different AF interactions J_1 and J_2 and F interaction J_3. A plateau at $m=1/6$ is obtained at small $|J_3|$; for fixed J_1 and J_2, the larger $|J_3|$ is, the narrower is the width of the plateau at $m=1/6$, and after $|J_3|$ exceeds a critical value, the plateau at $m=1/6$ is eventually smeared out; for fixed J_1 and J_3, the larger J_2 is, the wider is the width of the plateau at $m=1/6$; the saturated field is obviously unchanged with the changing F interaction J_3. The coupling dependence of the spin-1/2 nonfrustrated diamond chain with AF interactions J_1 and J_2 and F interaction J_3 is similar to that of trimerized F-F-AF chains.[25]

Figures 18(c) and 18(d) present the susceptibility χ as a function of temperature T for the spin-1/2 frustrated diamond chain with $J_1=1$, $J_3<0$, and $J_2=0.5$ and 2, where the external field is taken as $H/J_1=0.01$. A double-peak structure of $\chi(T)$ is observed at small F interaction $|J_3|$ and disappears at large $|J_3|$. The temperature dependence of the specific heat C with $J_1=1$, $J_3<0$, and $J_2=0.5$ and 2 is shown in Figs. 18(e) and 18(f), where $H/J_1=0.01$. It is seen that, when J_2 is small, $C(T)$ exhibits only a single peak; when J_2 is large, a double-peak structure of $C(T)$ is observed. In the latter case, the double-peak structure is more obvious for small F interaction $|J_3|$ and tends to disappear at large $|J_3|$. Therefore, the thermodynamics demonstrate various behaviors with different AF interactions J_1 and J_2 and F interaction J_3.

C. Effect of anisotropy of bond interactions

Some magnetic materials show different behaviors under longitudinal and transverse magnetic fields, showing that the anisotropy plays an important role in the physical properties of the system. First, let us investigate the XXZ anisotropy of

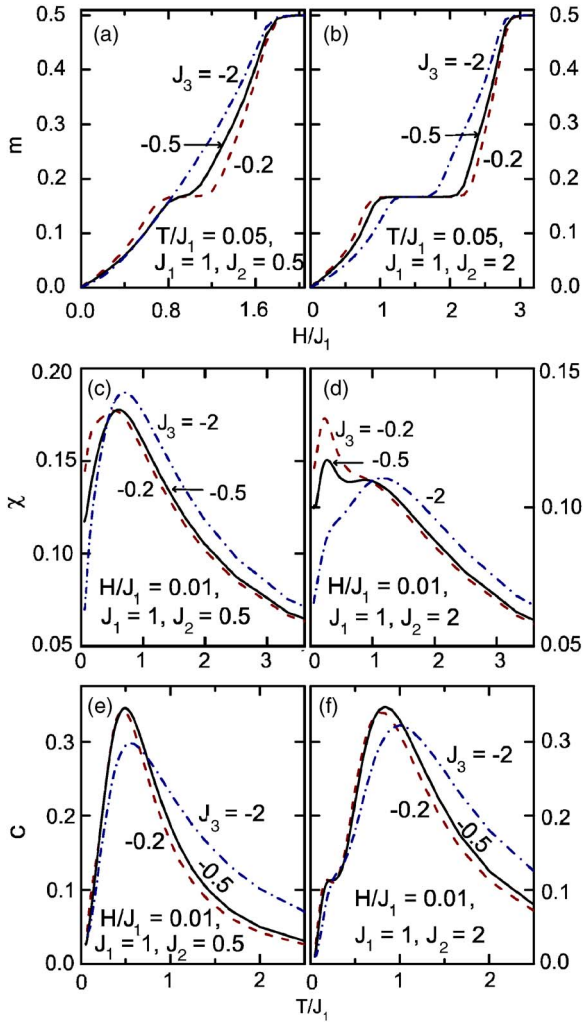

FIG. 18. (Color online) For the spin-1/2 nonfrustrated Heisenberg diamond chains with $J_1=1$ and $J_3<0$, the magnetization process $m(H)$ at temperature $T/J_1=0.05$ with (a) $J_2=0.5$ and (b) $J_2=2$; the susceptibility $\chi(T)$ at field $H/J_1=0.01$ with (c) $J_2=0.5$ and (d) $J_2=2$; the specific heat $C(T)$ at field $H/J_1=0.01$ with (e) $J_2=0.5$ and (f) $J_2=2$.

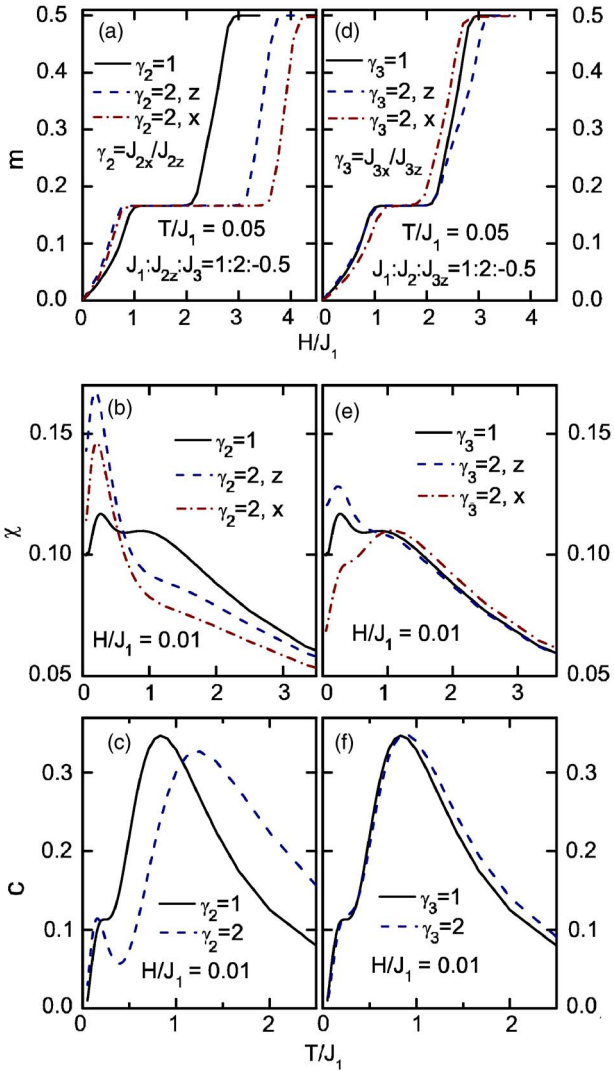

FIG. 19. (Color online) For the spin-1/2 nonfrustrated diamond chain with the couplings satisfying $J_1:J_{2z}:J_3=1:2:-0.5$ for various anisotropy $\gamma_2=J_{2x}/J_{2z}\geqslant 1$: (a) the magnetization process $m(H)$ at temperature $T/J_1=0.05$, (b) the susceptibility $\chi(T)$ at field $H/J_1=0.01$, and (c) the specific heat $C(T)$ at field $H/J_1=0.01$. For the spin-1/2 nonfrustrated diamond chain with couplings $J_1:J_2:J_{3z}=1:2:-0.5$ for various anisotropy $\gamma_3=J_{3x}/J_{3z}\geqslant 1$: (d) the magnetization process $m(H)$ at temperature $T/J_1=0.05$, (e) the susceptibility $\chi(T)$ at field $H/J_1=0.01$, and (f) the specific heat $C(T)$ at field $H/J_1=0.01$.

the AF interaction J_2 on the properties of the spin-1/2 nonfrustrated diamond chain with the couplings $J_1:J_{2z}:J_3=1:2:-0.5$ for various anisotropy parameter defined by $\gamma_2=J_{2x}/J_{2z}=J_{2y}/J_{2z}$, where the z axis is presumed to be perpendicular to the chain direction. For $\gamma_2\geqslant 1$, the magnetization $m(H)$, susceptibility $\chi(T)$, and specific heat $C(T)$ are presented in Figs. 19(a)–19(c), respectively. With increasing γ_2, it is found that when the magnetic field H is along the z direction, the width of the magnetization plateau at $m=1/6$ as well as the saturation field are enlarged, while these are more increased for H along the x direction than along the z direction. The peak of the susceptibility $\chi(T)$ for H along the z direction at the lower-temperature side is promoted, and the second round peak at the high-temperature side is depressed with a little shift, while $\chi(T)$ for H along the x direction shows the similar varying trend. The peak of the specific heat $C(T)$ for H along the z direction at the lower-temperature side is almost unchanged, and the second round peak at the high-temperature side moves towards the higher-temperature side, while $C(T)$ for H along the x direction coincides with those for H along the z direction. For $0<\gamma_2<1$, the anisotropy just shows the very reverse effect on the thermodynamic properties in comparison to what we discussed above.

Now, let us discuss the effect of the XXZ anisotropy of $J_3<0$ on the magnetic and thermodynamic properties of the spin-1/2 nonfrustrated diamond chain with the couplings $J_1:J_2:J_{3z}=1:2:-0.5$. Recall that as the J_2 bond connects two different lattice sites, as shown in Fig. 1, J_1 and J_3 can be different, even in their signs. Define a parameter γ_3 to characterize the anisotropy as $\gamma_3=J_{3x}/J_{3z}=J_{3y}/J_{3z}$, where the z axis is perpendicular to the chain direction. For $\gamma_3\geqslant 1$, the

magnetization $m(H)$, susceptibility $\chi(T)$, and specific heat $C(T)$ are depicted in Figs. 19(d), 19(e), and 19(f), respectively. With increasing γ_3, it is seen that the width of the plateau at $m=1/6$ for H along the z direction becomes slightly wider, while it goes smaller for H along the x direction. The saturation field is not changed with γ_3 along both directions. The peak of $\chi(T)$ for H along the z direction at the lower-temperature side is promoted, and the second round peak at the higher-temperature side is slightly depressed, while the situations along the x direction are just the reverse; namely, the peak at the lower-temperature side is depressed, and the second peak at the higher-temperature side is slightly promoted. The peak of $C(T)$ for H along the z direction at the lower-temperature side is almost unchanged, and the second round peak at the higher-temperature side moves slightly to the higher-temperature side, while $C(T)$ along the x direction coincides with that along the z direction. For $0<\gamma_3<1$, the situation just becomes the reverse of what we discussed above.

D. Comparison to experimental results

Recently, Kikuchi *et al.*[6] have performed a nice measurement on a spin-1/2 diamond-chain compound $Cu_3(CO_3)_2(OH)_2$, i.e., azurite. They have observed the 1/3 magnetization plateau, unambiguously confirming the previous theoretical prediction. The two broad peaks, both in the magnetic susceptibility and the specific heat, are observed. We note that in Ref. 6, the experimental data at finite temperatures are fitted by the zero-temperature theoretical results obtained by the exact diagonalization and DMRG methods, while the result of the high-temperature series expansion fails to fit the low-temperature behavior of the susceptibility. In accordance with our preceding discussions, by using the TMRG method, we have attempted to reanalyze the experimental data presented in Ref. 6 to fit the experiments for the whole available temperature region.

Our fitting results for the temperature dependence of the susceptibility χ of the compound $Cu_3(CO)_2(OH)_2$ are presented in Fig. 20(a). For a comparison, we have also included the TMRG result calculated by using the parameters given in Ref. 6. Obviously, our TMRG results with $J_1:J_2:J_{3z}=1:1.9:-0.3$ and $J_{3x}/J_{3z}=J_{3y}/J_{3z}=1.7$ fit very well the experimental data of χ, and the two round peaks at low temperatures are nicely reproduced, while the result with $J_1:J_2:J_3=1:1.25:0.45$ obtained in Ref. 6 cannot fit the low-temperature behavior of χ.[26] On the other hand, the fitting results for the temperature dependence of the specific heat $C(T)$ of the compound $Cu_3(CO)_2(OH)_2$ are shown in Fig. 20(b). The lattice contribution, which is included in the raw experimental data in Ref. 6, is subtracted according to $C(T)=C_{expt}(T)-\alpha T^3$, where α is a parameter. Obviously, our TMRG result with the same set of parameters $J_1:J_2:J_{3z}=1:1.9:-0.3$ and $J_{3x}/J_{3z}=J_{3y}/J_{3z}=1.7$ fits also remarkably well the experimental data of $C(T)$, and the two round peaks at low temperatures are nicely reproduced, while the result with $J_1:J_2:J_3=1:1.25:0.45$ given in Ref. 6 cannot fit the low-temperature behavior of $C(T)$, even qualitatively. In addition, the sharp peak of $C(T)$ experimentally observed at

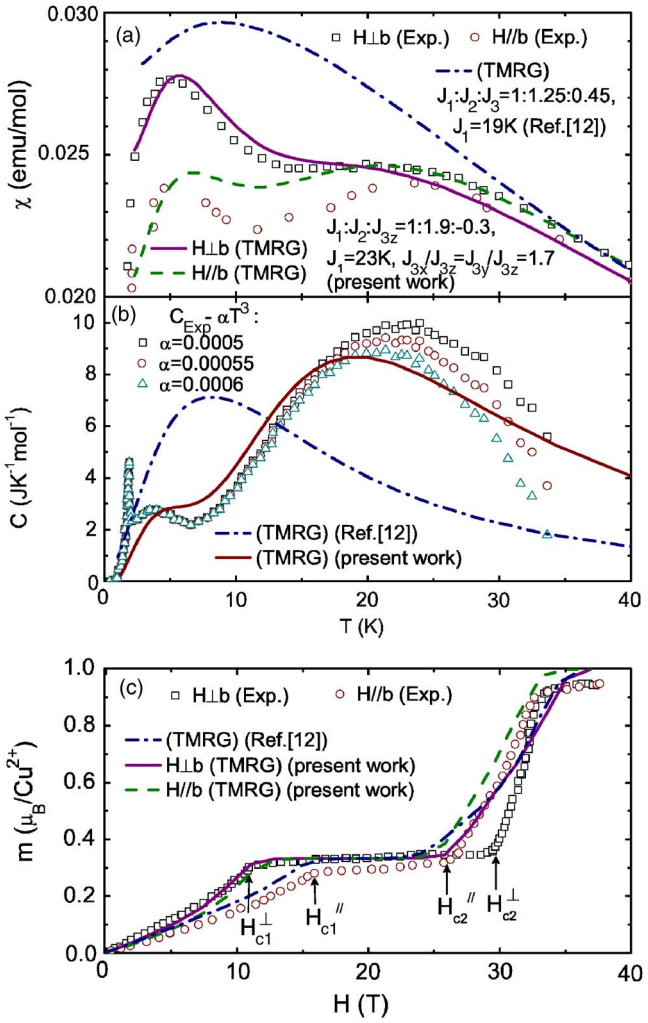

FIG. 20. (Color online) Comparison of experimental results for (a) the magnetic susceptibility, (b) the specific heat, and (c) the magnetization process for the spin-1/2 diamond compound $Cu_3(CO)_2(OH)_2$ with the TMRG results. The experimental data are taken from Ref. 6. See the context for details.

temperature around 2 K cannot be reproduced by both sets of the coupling parameters, which might be a three-dimensional long-range ordering due to interchain interactions. The fitting results for the magnetization $m(H)$ of the compound $Cu_3(CO)_2(OH)_2$ are shown in Fig. 20(c). We would like to point out that the quantitative fitting by our above parameters to the width of the plateau is not so good, but the qualitative behavior is quite consistent with the experiments both in the transverse and longitudinal magnetic fields, say, $H_{c1}^{\parallel}>H_{c1}^{\perp}$ and $H_{c2}^{\parallel}<H_{c2}^{\perp}$, and the saturation field is fixed along both directions, suggesting that our fitting parameters capture the main characteristics. It is worth pointing out that if the anisotropy ratio is increased up to $J_{3x}/J_{3z}=J_{3y}/J_{3z}=2.5$ with the same couplings $J_1:J_2:J_{3z}=1:1.9:-0.3$, the width of the 1/3 plateau for $H\|b$ will be decreased to about one-half of that for $H\perp b$.

Therefore, our calculations show that (i) the best couplings obtained by fitting the experimental data of the susceptibility for the azurite could be $J_1:J_2:J_{3z}=1:1.9:-0.3$

with the anisotropic ratio for the ferromagnetic interaction $J_{3x}/J_{3z}=J_{3y}/J_{3z}=1.7$, where $z\perp b$; (ii) the compound may not be a spin frustrated magnet; (iii) the double peaks of the susceptibility and the specific heat are not caused by the spin frustration effect, but by the two kind of gapless and gapful excitations owing to the competition of the AF and F interactions.

One might argue that for this diamond-chain compound, from the point of the lattice distance it is unlikely that J_1 is AF without an *XXZ* anisotropy while J_3 is F with a strong *XXZ* anisotropy. We may offer another possibility to support our findings, namely, that the case of J_1 and J_3 with opposite signs is not excluded from the lattice structure of the compound. A linear relationship exists between the exchange energy and the metal-ligand-metal bridge angle: the coupling energy, positive (ferromagnetic) at angles near 90°, becomes increasingly smaller (more antiferromagnetic) as the angle increases.[27] As the ferromagnetic coupling J_3 is determined by fitting the experimental low-temperature behaviors of $\chi(T)$ and $C(T)$, this fitting coupling parameters should not be impossible if one considers the angle of the J_1 bridge to keep the antiferromagnetic coupling and the angle of the J_3 bridge to induce the ferromagnetic coupling. On the other hand, we note that there is another compound with Cu ions, $Cu_2(abpt)(SO_4)_2(H_2O)\cdot H_2O$, whose g factors in the XY plane are different from that in the z direction.[28] Besides, someone might argue that the condition $J_2 \gg J_1, |J_3|$ is necessary to explain the double-peak behavior of the diamond chain. In fact, such an argument is not necessarily true, as manifested in Fig. 18(c), where the double peaks of $\chi(T)$ at low temperatures can also be produced with the parameters $J_1:J_2:J_3=1:0.5:-0.1$. In other words, the double-peak behavior of the diamond chain may not depend on whether $J_2 \gg J_1$, J_3 or not, but may be strongly dependent on the competition of AF and F interactions, as discussed above.

VI. SUMMARY AND DISCUSSION

In this paper, we have numerically studied the magnetic and thermodynamic properties of spin-1/2 Heisenberg diamond chains with three different cases: (a) J_1, J_2, $J_3>0$ (frustrated), (b) J_1, $J_3<0$, $J_2>0$ (frustrated), and (c) J_1, $J_2>0$, $J_3<0$ (nonfrustrated) by means of the DMRG and TMRG methods. In the ground states, the local magnetic moment, spin-correlation function, and static structure factor are explored. The static structure factor $S(q)$ at zero field shows peaks at wave vector $q=0$, $\pi/3$, $2\pi/3$, π, $4\pi/3$, and $5\pi/3$ for different couplings, in which the peaks at $q=0$, $2\pi/3$, and $4\pi/3$ in the magnetization plateau state with $m=1/6$ are observed to be coupling independent. The DMRG results of the zero-field static structure factor can be nicely fitted by a linear superposition of six modes, where two fitting equations are proposed. It is seen that the six modes are closely related to the low-lying excitations of the system. At finite temperatures, the magnetization, susceptibility, and specific heat are calculated, which show various behaviors for different couplings. The double-peak structure of the susceptibility and specific heat can be procured, whose positions and heights are found to be dependent on competing couplings. It has been shown that the *XXZ* anisotropy of F and AF couplings can have a remarkable effect on the physical behaviors of the system. In addition, the experimental susceptibility, specific heat, and magnetization of the diamond-chain compound $Cu_3(CO)_2(OH)_2$ (Ref. 6) can be nicely fitted by our TMRG results.

For the spin-1/2 frustrated Heisenberg diamond chains with AF couplings J_1, J_2, and J_3, the magnetization plateau at $m=1/6$ in the ground state coincides with a perfect fixed sequence of the averaged local magnetic moment such as $\{\ldots,(S_a,S_a,S_b),\ldots\}$ with $2S_a+S_b=1/2$, which might be described by trimerized states. On the other hand, the static structure factor $S(q)$ shows peaks at wave vectors $q=0$, $\pi/3$ $(5\pi/3)$, and $2\pi/3$ $(4\pi/3)$ for different external fields and different AF couplings. We note that the similar behavior of $S(q)$ has been experimentally observed in the diamond-type compound $Sr_3Cu_3(PO_4)_4$.[20] In addition, the DMRG results of the zero-field static structure factor can be nicely fitted by a linear superposition of six modes. It is observed that the six modes are closely related to the low-lying excitations of the present case. At finite temperatures, the magnetization $m(H)$, susceptibility $\chi(T)$, and specific heat $C(T)$ demonstrate different behaviors at different AF couplings, say, the magnetization plateau at $m=1/6$ is observed whose width is found to be dependent on the couplings; the double-peak structure is observed for the susceptibility $\chi(T)$ and specific heat $C(T)$ as a function of temperature, and the heights and positions of the peaks are found to be dependent on the AF couplings.

For the spin-1/2 frustrated Heisenberg diamond chains with F couplings J_1 and J_3 and AF coupling J_2, the magnetization plateau at $m=1/6$ in the ground state corresponds to a perfect fixed sequence of the averaged local magnetic moment such as $\{\ldots,(S_a,S_b,S_b),\ldots\}$ with $S_a+2S_b=1/2$, which could be understood by trimerized states. The static structure factor $S(q)$ shows peaks also at wave vectors $q=0$, $\pi/3$ $(5\pi/3)$, and $2\pi/3$ $(4\pi/3)$ for different external fields and different F couplings J_1 and J_3 and AF coupling J_2, which is expected to be experimentally observed in the related diamond-type compound. In addition, the DMRG results of the zero-field static structure factor can be nicely fitted by a linear superposition of six modes with the fitting equations mentioned above. The six modes are closely related to the low-lying excitations of the system. At finite temperatures, the magnetization $m(H)$, susceptibility $\chi(T)$, and specific heat $C(T)$ demonstrate various behaviors for different couplings; namely, the magnetization plateau at $m=1/6$ is observed, whose width is found to depend on the couplings; the double-peak structure is also observed for the susceptibility $\chi(T)$ and specific heat $C(T)$, and the heights and positions of the peaks are found dependent on F couplings J_1 and J_3 and AF coupling J_2.

For the spin-1/2 nonfrustrated Heisenberg diamond chains with AF couplings J_1 and J_2 and F coupling J_3, the magnetization plateau at $m=1/6$ in the ground state coincides with a perfect fixed sequence of the averaged local magnetic moment such as $\{\ldots,(S_a,S_b,S_b),\ldots\}$ with $S_a+2S_b=1/2$, which could be understood by trimerized states. The static structure factor $S(q)$ is observed to exhibit the peaks at wave vectors $q=0$ and $2\pi/3$ $(4\pi/3)$ for different external

fields and different AF couplings J_1 and J_2 and F coupling J_3, which could be experimentally detected in the related diamond-type compound. In addition, it is found that the zero-field spin-correlation function $\langle S_j^z S_0^z \rangle$ is similar to that of the $S=1/2$ Heisenberg AF chain. At finite temperatures, the magnetization $m(H)$, susceptibility $\chi(T)$, and specific heat $C(T)$ are found to reveal different behaviors for different couplings, i.e., the magnetization plateau at $m=1/6$ is obtained, whose width is found to depend on the couplings. The double-peak structure is observed for the temperature dependence of the susceptibility $\chi(T)$ and specific heat $C(T)$, where the heights and positions of the peaks depend on different AF couplings J_1 and J_2 and F coupling J_3.

The effect of the anisotropy of the AF and F interactions on the physical properties of the nonfrustrated Heisenberg diamond chain is also investigated. For the case of the couplings satisfying $J_1:J_{2z}:J_3=1:2:-0.5$, when the anisotropic ratio $\gamma_2=J_{2x}/J_{2z}=J_{2y}/J_{2z}\neq 1$, it is found that the width of the plateau at $m=1/6$, the saturation field, and the susceptibility $\chi(T)$ show the same tendency, but quantitatively different, under the external field H along the z and x directions, while the specific heat $C(T)$ for H along the z direction coincides with that along the x direction. For the case of the couplings satisfying $J_1:J_2:J_{3z}=1:2:-0.5$, when the anisotropic ratio $\gamma_3=J_{3x}/J_{3z}=J_{3y}/J_{3z}\neq 1$, it is seen that the width of the plateau at $m=1/6$, the saturation field, and the susceptibility $\chi(T)$ exhibit the opposite trends for H along the z and x directions, while the specific heat $C(T)$ for H along the z direction also coincides with that along the x direction.

For all the three cases, plateau states of $m=1/6$ are observed during the magnetization, whose static structure factor $S(q)$ shows peaks at wave vectors $q=0$, $2\pi/3$, and $4\pi/3$. But in the absence of the magnetic field, the static structure factor $S(q)$ in the ground state displays peaks at $q=0$, $\pi/3$, $2\pi/3$, π, $4\pi/3$, and $5\pi/3$ for the frustrated case with J_1, J_2, and $J_3>0$; peaks at $q=0$, $\pi/3$, π, and $5\pi/3$ for the frustrated case with J_1, $J_3<0$, and $J_2>0$; and a peak at $q=\pi$ for the nonfrustrated case with J_1, $J_2>0$, and $J_3<0$. In addition, the DMRG results of the zero-field static structure factor can be nicely fitted by a linear superposition of six modes, where the fitting equation is proposed. At finite temperatures, the double-peak structure of the susceptibility and specific heat against temperature can be obtained for all the three cases. It is found that the susceptibility shows ferrimagnetic characteristics for the two frustrated cases with some couplings, while no ferrimagnetic behaviors are observed for the nonfrustrated case.

The compound $Cu_3(CO)_2(OH)_2$ is regarded as a model substance for the spin-1/2 Heisenberg diamond chain. The 1/3 magnetization plateau and the two broad peaks both in the magnetic susceptibility and the specific heat have been observed experimentally.[6] Our TMRG calculations with $J_1:J_2:J_{3z}=1:1.9:-0.3$ and $J_{3x}/J_{3z}=J_{3y}/J_{3z}=1.7$ capture well the main characteristics of the experimental susceptibility, specific heat, and magnetization, indicating that the compound $Cu_3(CO)_2(OH)_2$ may not be a spin frustrated magnet.[26]

ACKNOWLEDGMENTS

We are grateful to D. P. Arovas for useful communication. This work is supported in part by the National Science Fund for Distinguished Young Scholars of China (Grant No. 10625419), the National Science Foundation of China (Grant Nos. 90403036, 20490210), and the MOST of China (Grant No. 2006CB601102).

APPENDIX: LOW-LYING EXCITATIONS OF SPIN-1/2 FRUSTRATED HEISENBERG DIAMOND CHAINS

In this appendix, the low-lying excitations of the spin-1/2 frustrated Heisenberg diamond chain are investigated by means of the Jordan-Wigner (JW) transformation. The Hamiltonian of the system reads

$$\mathcal{H}=\sum_{i=1}^{N}(J_1\mathbf{S}_{3i-2}\cdot\mathbf{S}_{3i-1}+J_2\mathbf{S}_{3i-1}\cdot\mathbf{S}_{3i}+J_3\mathbf{S}_{3i-2}\cdot\mathbf{S}_{3i}+J_3\mathbf{S}_{3i-1}\cdot\mathbf{S}_{3i+1}+J_1\mathbf{S}_{3i}\cdot\mathbf{S}_{3i+1})-H\sum_{j=1}^{3N}S_j^z, \tag{A1}$$

where $3N$ is the total number of spins in the diamond chain, $J_i>0$ $(i=1,2,3)$ represent the AF coupling while $J_i<0$ the F interaction, and H is the external magnetic field along the z direction. In accordance with the spin configuration of the diamond chain, we start from the JW transformation with spinless fermions,

$$S_j^+=a_j^+\exp\left(i\pi\sum_{m=1}^{j-1}a_m^+a_m\right),$$

$$S_j^z=a_j^+a_j-\frac{1}{2}, \tag{A2}$$

where $j=1,\ldots,3N$. Because the period of the present system is 3, three kinds of fermions in moment space can be introduced through the Fourier transformations

$$a_{3i-2}=\frac{1}{\sqrt{N}}\sum_k e^{ik(3i-2)}a_{1k},$$

$$a_{3i-1}=\frac{1}{\sqrt{N}}\sum_k e^{ik(3i-1)}a_{2k},$$

$$a_{3i}=\frac{1}{\sqrt{N}}\sum_k e^{ik(3i)}a_{3k}. \tag{A3}$$

Ignoring the interactions between fermions, the Hamiltonian takes the form of

$$H=E_0+\sum_k[(\omega_1a_{1k}^+a_{1k}+\omega_2a_{2k}^+a_{2k}+\omega_3a_{3k}^+a_{3k})+(\gamma_1a_{1k}a_{2k}^++\gamma_2a_{2k}a_{3k}^++\gamma_3a_{3k}a_{1k}^++\text{H.c.})], \tag{A4}$$

where $E_0=\frac{N}{4}(2J_1+J_2+2J_3-6H)$, $\omega_1=-(J_1+J_3)-H$, $\omega_2=-\frac{1}{2}(J_1+J_2+J_3)-H$, $\omega_3=\omega_2$, $\gamma_1=(J_1e^{ik}+J_3e^{-i2k})/2$, $\gamma_2=(J_2e^{ik})/2$, and $\gamma_3=(J_3e^{ik}+J_1e^{-ik})/2$.

Via the Bogoliubov transformation

$$a_{1k} = u_{11}(k)\alpha_{1k} + u_{12}(k)\alpha_{2k} + u_{13}(k)\alpha_{3k},$$

$$a_{2k} = u_{21}(k)\alpha_{1k} + u_{22}(k)\alpha_{2k} + u_{23}(k)\alpha_{3k},$$

$$a_{3k} = u_{31}(k)\alpha_{1k} + u_{32}(k)\alpha_{2k} + u_{33}(k)\alpha_{3k}, \tag{A5}$$

the Hamiltonian can be diagonalized as

$$H = E_g + \sum_k \sum_{i=1}^{3} \epsilon_{ik}\alpha_{ik}^{+}\alpha_{ik}. \tag{A6}$$

The coefficients of the Bogoliubov transformation can be found through equations of motion $i\hbar\dot{a}_{ik}=[a_{ik},H]$,

$$\begin{pmatrix} \omega_1 & \gamma_1 & \gamma_3 \\ \gamma_1^{*} & \omega_2 & \gamma_2 \\ \gamma_3^{*} & \gamma_2^{*} & \omega_3 \end{pmatrix} \begin{pmatrix} u_{1i} \\ u_{2i} \\ u_{3i} \end{pmatrix} = \epsilon_{ik} \begin{pmatrix} u_{1i} \\ u_{2i} \\ u_{3i} \end{pmatrix}. \tag{A7}$$

For a given k, the eigenvalues ε_{ik} and eigenvectors (u_{1i},u_{2i},u_{3i}) can be numerically calculated by the driver *ZGEEV.f* of the *LAPACK*, which is available on the website.[29] Figure 7 shows the zero-field low-lying fermionic excitation $\varepsilon(k)$ for the frustrated diamond chain with different AF couplings, while Fig. 13 presents the zero-field low-lying fermionic excitation $\varepsilon(k)$ for the frustrated diamond chain with J_1, $J_3<0$, and $J_2>0$.

*Corresponding author. Electronic address: gsu@gucas.ac.cn

[1] M. Oshikawa, M. Yamanaka, and I. Affleck, Phys. Rev. Lett. **78**, 1984 (1997).
[2] M. Drillon, E. Coronado, M. Belaiche, and R. L. Carlin, J. Appl. Phys. **63**, 3551 (1988); M. Drillon, M. Belaiche, P. Legoll, J. Aride, A. Boukhari, and A. Moqine, J. Magn. Magn. Mater. **128**, 83 (1993).
[3] H. Sakurai, K. Yoshimura, K. Kosuge, N. Tsujii, H. Abe, H. Kitazawa, G. Kido, H. Michor, and G. Hilscher, J. Phys. Soc. Jpn. **71**, 1161 (2002).
[4] M. Ishii, H. Tanaka, M. Mori, H. Uekusa, Y. Ohashi, K. Tatani, Y. Narumi, and K. Kindo, J. Phys. Soc. Jpn. **69**, 340 (2000).
[5] M. Fujisawa, J. Yamaura, H. Tanaka, H. Kageyama, Y. Narumi, and K. Kindo, J. Phys. Soc. Jpn. **72**, 694 (2003).
[6] H. Kikuchi, Y. Fujii, M. Chiba, S. Mitsudo, T. Idehara, T. Tonegawa, K. Okamoto, T. Sakai, T. Kuwai, and H. Ohta, Phys. Rev. Lett. **94**, 227201 (2005).
[7] H. Kikuchi, Y. Fujii, M. Chiba, S. Mitsudo, and T. Idehara, Physica B **329**, 967 (2003).
[8] K. Takano, K. Kubo, and H. Sakamoto, J. Phys.: Condens. Matter **8**, 6405 (1996).
[9] K. Okamoto, T. Tonegawa, Y. Takahashi, and M. Kaburagi, J. Phys.: Condens. Matter **11**, 10485 (1999).
[10] T. Tonegawa, K. Okamoto, T. Hikihara, Y. Takahashi, and M. Kaburagi, J. Phys. Soc. Jpn. **69**, 332 (2000).
[11] K. Sano and K. Takano, J. Phys. Soc. Jpn. **69**, 2710 (2000).
[12] T. Tonegawa, K. Okamoto, T. Hikihara, Y. Takahashi, and M. Kaburagi, J. Phys. Chem. Solids **62**, 125 (2001).
[13] K. Okamoto, T. Tonegawa, and M. Kaburagi, J. Phys.: Condens. Matter **15**, 5979 (2003).
[14] A. Honecker and A. Lauchli, Phys. Rev. B **63**, 174407 (2001).
[15] D. D. Swank and R. D. Willett, Inorg. Chim. Acta **8**, 143 (1974).
[16] S. White, T. Xiang, and X. Wang, *Density-Matrix Renormalization*, Lecture Notes in Physics Vol. 528, edited by I. Peschel, X. Wang, M. Kaulke and K. Hallberg (Springer-Verlag, New York, 1999).
[17] U. Schollwock, Rev. Mod. Phys. **77**, 259 (2005).
[18] We have checked that in the present situation, the static structure factor $S(q)$ calculated from $\langle S_j^z S_0^z\rangle$ coincides with that from $\langle(S_j^z-\langle S_j^z\rangle)(S_0^z-\langle S_0^z\rangle)\rangle$.
[19] Y. Ajiro, T. Asano, K. Nakaya, M. Mekata, K. Ohoyama, Y. Yamaguchi, Y. Koike, Y. Morii, K. Kamishima, H. A. Katori, and T. Goto, J. Phys. Soc. Jpn. **70**, 186 (2001).
[20] D. P. Arovas, A. Auerbach, and F. D. M. Haldane, Phys. Rev. Lett. **60**, 531 (1988).
[21] The system under interest involves possibly ferrimagnetic, dimerized, and spin liquid phases, leading to the spin-spin-correlation functions exhibiting different behaviors including exponential or power-law decaying. The constant c_l in Eq. (7) characterizes the long-range order in ferrimagnetic phase.
[22] B. Gu, G. Su, and S. Gao, Phys. Rev. B **73**, 134427 (2006).
[23] I. Affleck, D. Gepner, H. J. Schulz, and T. Ziman, J. Phys. A **22**, 511 (1989).
[24] R. R. P. Singh, M. E. Fisher, and R. Shanker, Phys. Rev. B **39**, 2562 (1989).
[25] B. Gu, G. Su, and S. Gao, J. Phys.: Condens. Matter **17**, 6081 (2005).
[26] B. Gu and G. Su, Phys. Rev. Lett. **97**, 089701 (2006).
[27] J. C. Livermore, R. D. Willett, R. M. Gaura, and C. P. Landee, Inorg. Chem. **21**, 1403 (1982).
[28] P. J. van Koningsbruggen, D. Gatteschi, R. A. G. de Graaff, J. G. Haasnoot, J. Reedijk, and C. Zanchini, Inorg. Chem. **34**, 5175 (1995).
[29] http://www.netlib.org/lapack/